https://doi.org/10.5194/essd-2026-850
Preprint. Discussion started: 13 November 2026
© Author(s) 2026. CC BY 4.0 License.



Open Access Earth System Science Data Discussions

High spatial resolution emissions inventory (2005-2022) in Chile from livestock and waste sectors

Diana Rojas[1], Nicolás Álamos[1-2], Nicolás Huneeus[1-2], Mariel Opazo[1-2-4], Ignacio Leiva[1-2], Kevin Basoa[4], Ignacio Beltrán[4-5], Tia Scarpelli[6], Mauricio Osses[2-3], Juan Pablo Boisier[1-2].

[1]Department of Geophysics (DGF), Universidad de Chile, Santiago, Chile
[2]Center for Climate and Resilience Research (CR2), Santiago, Chile
[3]Department of Mechanical Engineering, Universidad Técnica Federico Santa María (USM), Valparaíso, Chile
[4]Ministry of the Environment, Santiago, Chile
[5]Agricultural Research Institute (INIA), Chile
[6]Carbon Mapper, Pasadena, California, USA

Correspondence to: Diana Rojas (dianar.vergara.drv@gmail.com)

Abstract

Methane (CH_4) is a critical short-lived climate forcer (SLCF), and emissions inventories provide key information to mitigate its impact. The agricultural and waste sectors are among the most significant global anthropogenic sources of CH_4 and other atmospheric species, yet in Chile, the national greenhouse gas inventory reports them only at the regional (administrative) level. Here methane, together with other greenhouse gases and air quality pollutants from agricultural livestock, solid waste disposal, and wastewater treatment and discharge, was estimated at high spatial resolution as part of the high-resolution national inventory of anthropogenic emissions (INEMA). Annual emissions of CH_4, nitrous oxide (N_2O), ammonia (NH_3), and non-methane volatile organic compounds (NMVOCs) were quantified for 2005–2022, using national activity data, country-specific emission factors where available, and national spatial proxies. Over this period, combined CH_4 emissions rose by about 37 % to 574 Gg in 2022, dominated by solid waste disposal and livestock enteric fermentation, while livestock manure management was the main source of N_2O, NH_3, and NMVOC. Emissions concentrate in the central and southern zones of the country, consistent with previous inventories; however, the high resolution of INEMA resolves the specific sources behind these patterns, distinguishing diffuse pasture-based livestock emissions in the south from discrete waste disposal point sources in the central zone. By identifying the specific sources that dominate national emissions, notably a small number of high-emitting waste-disposal sites, the updated INEMA dataset (version 3.0, which integrates these livestock and waste sectors into the full national inventory; available at https://doi.org/10.5281/zenodo.23169719, Álamos Correa et al., 2026) supports atmospheric modelling, complements national and global emissions inventories, and informs targeted public policies.

https://doi.org/10.5194/essd-2026-850
Preprint. Discussion started: 13 November 2026
© Author(s) 2026. CC BY 4.0 License.



Open Access Earth System Science Data Discussions

1. Introduction

Methane (CH_4) is a short-lived climate forcer (SLCF) and a potent greenhouse gas (GHG), with a global warming potential about 28 times that of carbon dioxide (CO_2) over a 100-year time horizon (IPCC, 2021). CH_4 has received increasing attention in emission inventories, due to its role in driving near-term climate change (Saunois et al., 2025; UNEP/CCAC, 2021). At global scale, atmospheric CH_4 concentrations have increased, driven by rising anthropogenic emissions originating primarily from agriculture (e.g., livestock production, rice cultivation, and biomass burning), fossil fuel production and use, and waste disposal (Saunois et al., 2025). In this context, high resolution emissions inventories provide the technical foundation for identifying major emission sources, characterizing air quality, and designing targeted public policies. Additionally, developing country-specific information is essential to reconcile the discrepancies documented between global emissions products and national realities in South America (Huneeus et al., 2020, Puliafito et al., 2021; Castesana et al., 2018).

In Chile, the National Greenhouse Gas Inventory (INGEI, from the Spanish *Inventario Nacional de Gases de Efecto Invernadero*) provides a bottom-up perspective of sectoral emissions at a regional scale as part of the reporting obligations under the United Nations Framework Convention on Climate Change (UNFCCC, 2023). However, these reports often lack the spatial granularity required for local-scale applications, highlighting a critical need for spatially explicit datasets to better understand the distribution of these emissions. To address this gap, the High-Resolution Inventory of Anthropogenic Emissions (INEMA, from the Spanish *Inventario Nacional de emisiones Antropogénicas*) was developed (Álamos et al., 2022). Nevertheless, the current version of INEMA does not yet include the agricultural and waste sectors, which represent a significant void in the national methane budget. Emissions from these sectors depend strongly on local conditions and specific practices such as climate, production systems, manure management systems, waste composition, and treatment technologies (IPCC, 2006; 2019).

Within the agricultural sector, CH_4 emissions are generated primarily through enteric fermentation in ruminants and, to a lesser extent, through manure management systems; together, these sectors account for approximately 25–40 % of global anthropogenic methane emissions (Dangal et al., 2017; Reisinger et al., 2021). Furthermore, additional emissions of nitrous oxide (N_2O), ammonia (NH_3), and non-methane volatile organic compounds (NMVOCs) are also produced in the manure management process (IPCC, 2006; EMEP/EEA, 2023). In contrast, the waste sector, which includes solid waste disposal, biological treatment, open burning and incineration, and wastewater treatment and discharge (IPCC, 2006), accounts for approximately 18 % of global anthropogenic CH_4 emissions (Bogner et al., 2008). While other pollutants and trace gases are released from this sector, their contributions are generally considered minor compared to methane (EMEP/EEA, 2023).

https://doi.org/10.5194/essd-2026-850
Preprint. Discussion started: 13 November 2026
© Author(s) 2026. CC BY 4.0 License.



In Chile, the most significant sources of CH_4 are livestock enteric fermentation and solid waste disposal (MMA, 2024a). Livestock production is a key component of Chile's economy (ODEPA, 2024), with cattle being the primary species contributing to these emissions. The sector exhibits marked geographical variability, with intensive dairy systems concentrated in the central-south regions and extensive beef production spanning the southern territories. Simultaneously, solid waste disposal has increased significantly, driven by population and economic growth (Cayumil et al., 2021; Kaza et al., 2018). In 2019, Chile generated approximately 18 million tons of non-hazardous waste, including both organic and inorganic fractions (MMA, 2023). Approximately 50 % of this total originated from the industrial sector and 48 % from municipal sources, while the remainder corresponds mainly to wastewater treatment sludge.

This study aims to estimate high-resolution (0.01° x 0.01°) emissions for the livestock and waste sectors in Chile for the period 2005-2022. This work serves as an extension of the INEMA inventory, which provides a sectoral and spatial dataset for both greenhouse gases and air pollutants (Álamos et al., 2022). This comprehensive update incorporates previously unconsidered sources, enhancing the robustness of national information. By providing a detailed spatial representation, this inventory serves as a critical input for air quality modeling and offers a spatially explicit tool to complement the INGEI, enabling the detection of local hotspots and supporting the design of national mitigation strategies.

The remainder of this paper is organized as follows: Section 2 describes the datasets and methodologies applied to estimate emissions for each sector and pollutant; Section 3 presents the main results and spatial distribution patterns; Section 4 compares INEMA with other national and global inventories and with top-down observations to assess its robustness; Section 5 discusses the main advances, limitations, and future directions; and Section 6 summarizes the main conclusions.

2. Methodology and Data

INEMA is a high-resolution national anthropogenic emissions inventory developed for Chile to support climate and air quality assessments. The first version is described in Álamos et al. (2022), while a second version was subsequently released as a public dataset (https://zenodo.org/records/7970953). This second version includes emissions for the 2015-2020 period from energy production (1.A.1), industrial energy consumption (1.A.2), on-road transport energy consumption (1.A.3.b), commercial energy consumption (1.A.4.a), residential firewood consumption (1.A.4.b), agricultural energy consumption (1.A.4.c), industrial processes (2), and biomass burning (3.C.1), the latter of which treats agricultural waste and forest fires separately.

This study represents an extension of INEMA (version 3), specifically incorporating the livestock and waste sectors. This update includes enteric fermentation (3.A.1), manure management (3.A.2),

https://doi.org/10.5194/essd-2026-850
Preprint. Discussion started: 13 November 2026
© Author(s) 2026. CC BY 4.0 License.



solid waste disposal (4.A), and wastewater treatment and discharge (4.D), following the 2006 IPCC Guidelines for National Greenhouse Gas Inventories (IPCC, 2006). Annual emissions of CH_4, N_2O, NH_3 and NMVOCs were quantified at a 0.01° x 0.01° spatial resolution for the 2005-2022 period, reflecting the availability of national input data. The resulting version 3.0 of INEMA, archived on Zenodo (Álamos Correa et al., 2026; https://doi.org/10.5281/zenodo.23169719), therefore comprises the complete national inventory: the sectors released in the previous versions together with the livestock and waste sectors presented in this work. Parallel to this, Osses et al. (2022) developed detailed high-resolution road transport estimates for the 1990–2020 period, which serve as a critical input for the INEMA national grid.

Emission estimates in this study follow the general methodology of the 2006 IPCC Guidelines for National Greenhouse Gas Inventories and their 2019 Refinement (IPCC, 2006; 2019) for CH_4 and N_2O emissions, while the European Monitoring and Evaluation Programme/European Environment Agency guidebook (EMEP/EEA, 2023) was used to estimate NH_3 and NMVOC. Emissions were quantified only for sector–pollutant combinations for which methodologies are explicitly defined in the corresponding guidelines, as summarized in Table 1. Specifically, for the livestock sector, we followed IPCC Volume 4 (Chapters 10 and 11) and EMEP/EEA Section 3.B. For the waste sector, estimates were based on IPCC Volume 5 (Chapter 2, 3, and 6) and EMEP/EEA Sections 5.A and 5.D. Pollutants not covered by these specific methodologies were excluded from the inventory.

National sources of activity data (AD) and country-specific parameters were obtained from the institutions and databases listed below: National Greenhouse Gas Inventory (INGEI), the Ministry of the Environment (MMA), the Agricultural and Livestock Service (SAG), the Superintendence of Sanitary Services (SISS), the Pollutant Release and Transfer Register (RETC), the National Socioeconomic Characterization Survey (CASEN), Undersecretariat for Regional and Administrative Development (SUBDERE), Chilean Central Bank (BCC), Ministry of Social Development and Family of Chile (MDSF), Chile's National Institute of Statistics (INE). Additionally, datasets developed by the Center for Climate and Resilience Research (CR2) were used, including high-resolution land use change (CR2LUC, Boisier et al., 2024a) and high resolution water uses (CR2WU, Boisier et al., 2024b). Since each sector relies on specific data sources, the integration and processing of these datasets are detailed within their respective sections. All acronyms above are derived from their Spanish names and are detailed in the Supplementary Material (Sect. S1; Table S1), and the summary of each AD source is provided in the Supplementary Material (Sect. S2; Table S2.1).

Default emission factors (EF) and parameters were adopted from the corresponding guidelines (IPCC, 2006; 2019; EMEP/EEA, 2023), while country-specific EF, particularly for the livestock sector (e.g., emission factors, nitrogen excretion rates, manure management system distributions,

https://doi.org/10.5194/essd-2026-850
Preprint. Discussion started: 13 November 2026
© Author(s) 2026. CC BY 4.0 License.



typical animal mass), were taken from INGEI (MMA, 2024a). A summary of the sources of EF and other parameters is provided in Supplementary Material (Sect. S2; Tables S2.2 and S2.3).

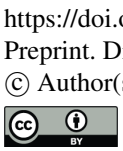
Table 1. IPCC sectors, pollutants, emission factor sources, and activity data used in this study.

IPCC Code	Sector	Pollutants	EF	Activity Data (AD)	Source of AD
3.A.1	Livestock—Enteric Fermentation	CH_4	Country-specific, IPCC 2019	Number of animals per commune	CR2WU (Boisier et al., 2024b)
3.A.2	Livestock—Manure Management	CH_4, NH_3, N_2O, NMVOC	Country-specific, IPCC 2019, EMEP/EEA 2023	Number of animals per commune	CR2WU (Boisier et al., 2024b)
4.A	Solid Waste Disposal	CH_4, NMVOC	Country-specific, IPCC 2019	Domestic and industrial waste generation	INGEI (MMA, 2024a) - RETC (MMA, 2024b)
4.D	Watewaster Discharge and Treatment	CH_4, NH_3, N_2O, NMVOC	Country-specific, IPCC 2019, EMEP/EEA 2023	Population coverage by disposal system and treated volume per plant	SISS 2024b - CASEN (MDSF, 2024)

2.1. Study area

Located in the southern cone of South America, Chile extends approximately 4,250 km from approximately 17°30’S to 56°30’S and has a population of about 19 million inhabitants, according to INE population projections (INE, 2017a). Administratively, the country is divided into 16 regions and 346 communes (the smallest administrative unit in Chile), which can be grouped into four macro-zones (Fig. 1) with distinct demographic, climatic, and geographic characteristics.

https://doi.org/10.5194/essd-2026-850
Preprint. Discussion started: 13 November 2026
© Author(s) 2026. CC BY 4.0 License.



Open Access Earth System Science Data Discussions

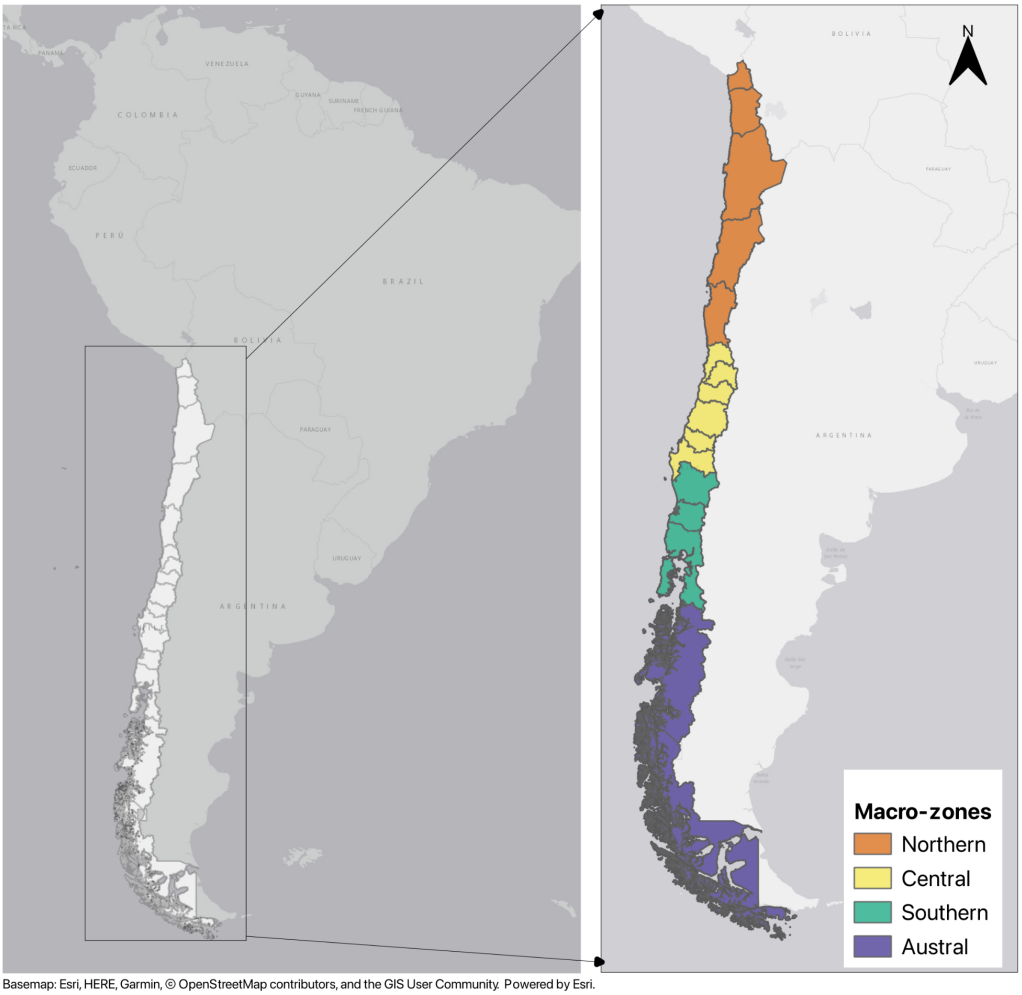


Figure 1. Map of continental Chile showing the four macro-zones defined in this study: Northern (red), Central (yellow), Southern (green), and Austral (blue). The boundaries of the 16 administrative regions of the country are indicated. The left panel shows Chile in the context of South America, while the right panel presents the macro-zone delineation within the country. Basemap: Esri World Light Gray Canvas. Sources: Esri, HERE, Garmin, © OpenStreetMap contributors, and the GIS User Community. Powered by Esri.

The northern macro-zone, extending approximately from 17°30'S to 32°10'S, includes the Atacama Desert and is dominated by arid and desert climates. The central macro-zone (32°10'S–38°45'S) is characterized by Mediterranean and temperate climates, while the southern macro-zone (38°45'S–44°00'S) exhibits temperate rainy conditions. Unlike previous versions of INEMA,

https://doi.org/10.5194/essd-2026-850
Preprint. Discussion started: 13 November 2026
© Author(s) 2026. CC BY 4.0 License.


the present study distinguishes an austral macro-zone, extending from 44°00'S to 56°30'S (Sarricolea et al., 2017), characterized by cold temperate and subpolar climates. The separation between the southern and austral macro-zones was introduced to better capture the spatial heterogeneity of emission sources across southern Chile, particularly in livestock and waste sectors, which exhibit strong contrasts in activity levels between the two areas.

2.2. Livestock

Enteric fermentation is the main source of CH_4 emissions in the livestock sector. It occurs during the microbial digestion of feed in animals, and it is particularly significant in ruminants, which have complex multi-chambered stomachs. The magnitude of these emissions varies according to animal species, age or physiological state, feed quality, and intake (FAO, 2023; IPCC, 2006).

Manure management constitutes an additional source of emissions. CH_4 and NMVOCs arise from the anaerobic decomposition of organic matter during manure storage and handling, while NH_3 is emitted through the volatilization of total ammoniacal nitrogen (TAN). N_2O emissions occur through nitrification and denitrification processes and are classified into direct emissions, which occur during storage and treatment, and indirect emissions, which result from nitrogen losses through volatilization and leaching. The magnitude and relative contribution of these emissions depend on production systems, feed intake, nitrogen excretion, storage conditions, and management practices (IPCC, 2019; EMEP/EEA, 2023).

2.2.1. Activity data:

Livestock population data, at the commune level, were obtained from CR2WU for the period 1950-2021 in continental Chile (Boisier et al., 2024b), which provides communal scale counts disaggregated by species. For 2022, livestock populations were estimated by carrying forward the 2021 values. The reference and access details for this dataset are provided in the Supplementary Material (Sect. S2; Table S2.1).

For this study, the available livestock species were grouped into dairy cattle and non-dairy cattle (e.g., beef cows, bulls, steers, and calves), swine, poultry, and other species (sheep, goats, horses, mules, llamas, and alpacas). Livestock were further classified into low-intensity grazing systems and high-intensity confinement systems, according to production practices and manure management characteristics (see Table 2). Under this framework, low-intensity systems were assumed to involve animals raised in grazing areas where manure is directly deposited on soils, whereas high-intensity systems involve manure collected and managed within production facilities. This classification determines the manure-management characterization of each species, detailed in the Supplementary Material (Sect. S2; Table S2.4), following the manure-management

https://doi.org/10.5194/essd-2026-850
Preprint. Discussion started: 13 November 2026
© Author(s) 2026. CC BY 4.0 License.



system distribution reported in INGEI (MMA, 2024a), while the corresponding spatial allocation (point sources for swine and poultry, and pastureland for dairy cattle) is described below.

Different spatial proxies were applied according to the production system. For low-intensity systems, yearly communal livestock populations were allocated within pasture areas based on the 1×1 km (i.e., 0.01° x 0.01°) yearly land cover CR2LUC dataset (Boisier et al., 2024a, see Supplementary Material, Sect. S2, Table S2.1). Since the CR2LUC land cover dataset covers the 1950–2020 period, the 2020 land cover was used as the spatial proxy for 2021 and 2022. For high-intensity swine and poultry systems, populations were allocated to point sources using establishment records obtained from SAG via Chilean Transparency Law request (SAG, 2024; Table S3.1). As these records do not include annual timestamps, the same spatial distribution of establishments was assumed across the entire study period. When establishment data were incomplete (accounting for about 1 % of livestock heads within high-intensity systems), the remaining livestock population was distributed following low-intensity system proxies. Dairy cattle, although managed under high-intensity systems, were spatially allocated to pasture areas at the commune level using the CR2LUC land-cover proxy described above, reflecting that dairy production in Chile occurs predominantly on grazing land.

Table 2. Livestock categories, production systems, spatial units, and species estimated.

Livestock type	Production system	Spatial Unit	Pollutant estimated
Swine Dairy Cattle Poultry*	High-intensity	Establishment and Pasture Land Cover	CH_4, N_2O, NMVOC, NH_3
Non-dairy cattle* Other species	Low-intensity	Pasture Land Cover	CH_4

**Poultry do not emit CH_4 from enteric fermentation; therefore, this pollutant was not estimated for this group. Note: N_2O, NH_3, and NMVOC emissions were estimated only for animals in confinement systems, namely swine, dairy cattle, poultry and the fraction of calves (within non-dairy cattle) managed in confinement. A small fraction (<1 %) lacking establishment-level information was assigned to the grazing system and excluded from these pollutants.*

2.2.2. Emission Estimation Methods

Methane emissions from enteric fermentation were quantified only for livestock species with relevant enteric processes (dairy and non-dairy cattle, swine, and other livestock). In contrast, CH_4 emissions from manure management were estimated for all livestock species. Emissions of N_2O, NH_3, and NMVOC from manure management were estimated only for livestock raised under high-

https://doi.org/10.5194/essd-2026-850
Preprint. Discussion started: 13 November 2026
© Author(s) 2026. CC BY 4.0 License.



intensity confinement systems (swine, dairy cattle and poultry, and the fraction of calves within non-dairy cattle managed under confinement). Emissions associated with manure deposited directly on pasture (low-intensity grazing system, see Table 2) are excluded from this study and will be incorporated in future INEMA versions under the agricultural soils sector, as recommended by the IPCC (2006). All emissions were estimated as annual totals; therefore, the time index is omitted in the following equations for brevity.

Enteric fermentation CH_4 emissions (LEF CH_4 in t yr^{-1}) were calculated as the product of emission factor (EF, kg $head^{-1}$ yr^{-1}) and the animal population (N) for each livestock type (T) and production system (P), where the factor 10^3 converts kilograms to tonnes. Following the Tier 2 approach, country-specific emission factors were applied for dairy and non-dairy cattle, as reported in the national inventory (MMA, 2024a). For the remaining livestock categories, a Tier 1 approach was used, applying default IPCC values due to the lack of national coefficients for those species. Specific references for all emission factors used are provided in the Supplementary Material (Section S2; Table S2.2). The calculation is described in Eq. (1):

$$LEF\ CH_4 = \sum_{T,P} EF_{(T,P)} \cdot \left(\frac{N_{(T,P)}}{10^3}\right) \quad (1)$$

Methane emissions from manure management (LMM CH_4) were estimated using two approaches based on data availability. For dairy cattle, non-dairy cattle and swine, a Tier 2 approach was adopted by applying country-specific emission factor (kg CH_4 $head^{-1}$ yr^{-1}) derived from the INGEI (MMA, 2024a). In these cases, emissions were calculated directly as the product of the emission factor and the corresponding animal population.

In contrast, a Tier 1 approach was used for the remaining livestock categories, applying default IPCC emission factors. For these species, emissions were estimated as the product of animal population (N), the volatile solids excreted per head (VS), the fraction of manure allocated to each management system (AWMS) and the default emission factor of the manure management system (EF), summed over each livestock type (T), production system (P), and manure management system (S), as shown in Eq. (2).

$$LMM\ CH_4 = \left[\sum_{T,S,P} \left(N_{(T,P)} \cdot VS_{(T,P)} \cdot AWMS_{(T,S,P)} \cdot EF_{T,S,P}\right)/1000\right] \quad (2)$$

Volatile solids excretion rates (VS) were derived from typical animal mass (TAM) values obtained from INGEI (MMA, 2024a) and default IPCC volatile solids excretion parameters. For poultry, we applied the IPCC high-productivity emission factor (solid storage) rather than the Latin American low-productivity default, reflecting Chile's predominantly industrial, confined poultry operations, with a broiler-representative TAM of 2.5 kg used to derive volatile solids. All specific references to these parameters, emissions factors, and the fractional distribution of the manure

https://doi.org/10.5194/essd-2026-850
Preprint. Discussion started: 13 November 2026
© Author(s) 2026. CC BY 4.0 License.



management systems are provided in the Supplementary Material, Section S2; Table S2.2, S2.3 and S2.4).

Direct N_2O emissions from manure management (LMM N_2O), which occur directly within storage and treatment systems via combined nitrification and denitrification processes, were estimated as a function of the animal population (N), the nitrogen excretion rate (Nex), the fraction of manure managed in each animal waste management system (AWMS), and the emission factor (EF). Emissions were subsequently converted to N_2O using the molecular weight ratio of 44/28, as shown in Eq. (3). Country-specific nitrogen excretion rates for dairy cattle were taken from the INGEI (MMA, 2024a), while default values were applied for swine and poultry. The specific references to these values are detailed in the Supplementary Material (Section S2; Tables S2.3). Default IPCC emission factors (EF) were applied for all species, and their sources are detailed in the Supplementary Material (Section S2; Table 2.2).

$$LMM\ N_2O = \left[\sum_S \left[\sum_{T,P} \left(\left(N_{(T,P)} \cdot Nex_{(T,P)}\right) \cdot AWMS_{(T,S,P)}\right)\right] \cdot EF_{(S)}\right] \cdot \frac{44}{28} \quad (3)$$

Indirect N_2O emissions, which result from the subsequent environmental conversion of nitrogen lost from the systems via volatilization (primarily as NH_3 and NO_x) and leaching or runoff, were calculated based on total nitrogen losses (N_{losses}) attributed to volatilization and leaching, multiplied by the corresponding emission factor (EF), and converted to N_2O using the 44/28 molecular weight ratio. Nitrogen losses were estimated as the product of the animal population (N), the nitrogen excretion rate (Nex), the fraction of manure managed in each system (AWMS), and the specific fraction of nitrogen lost via each pathway ($Frac_{losses}$), as shown in Eq. (4). Most of these variables are consistent with those used in previous calculations described above. Default IPCC values were applied for nitrogen loss fractions ($Frac_{losses}$) and for volatilization and leaching emission factors; the specific references for these parameters are consolidated in Supplementary Material (Section S2; Table S2.2 and S2.3).

$$N_{losses} = \left[\sum_S \left[\sum_{T,P} \left(\left(N_{(T,P)} \cdot Nex_{(T,P)} \cdot AWMS_{(T,S,P)}\right) + N_{cdg(s)}\right) \cdot Frac_{losses(T,S)}\right]\right] \quad (4)$$

Notably, losses via leaching were only accounted for from the Ñuble Region to the south (approximately south of 36°S). This geographic threshold reflects the climatic conditions required for leaching to occur, specifically where annual precipitation exceeds evapotranspiration, conditions that are generally not met in the arid and semi-arid regions of northern and central Chile.

Finally, NMVOC and NH_3 emissions were estimated as the product of the animal population and the corresponding default emission factors; references for these factors are provided in the

https://doi.org/10.5194/essd-2026-850
Preprint. Discussion started: 13 November 2026
© Author(s) 2026. CC BY 4.0 License.



Supplementary Material (Section S2; Table S2.2). It is important to note that these estimates were calculated independently for each pollutant; therefore, a full nitrogen mass-balance, ensuring strict consistency between NH_3 and N_2O pathways, was not performed. This approach follows the standard Tier 1 application of separate IPCC and EMEP/EEA guidelines.

2.3. Solid Waste Disposal

CH_4 and NMVOC are the most relevant pollutants associated with gas generation in solid waste disposal (SWD) sites. CH_4 generation occurs during the anaerobic decomposition of organic waste. This process begins shortly after waste deposition and can continue for several decades (IPCC, 2006). Thus, the estimation of current emissions must account for waste deposited in previous years. The First Order Decay (FOD) model, recommended by the IPCC, is widely used to simulate the time-dependent degradation of degradable organic carbon and the gradual release of CH_4 (IPCC, 2006; Malmir et al., 2023; Merab et al., 2025). The magnitude of CH_4 production depends on waste composition, climate, moisture content, and site management conditions (IPCC, 2019; Ishigaki et al., 2005; Spokas et al., 2003).

NMVOC is released in much smaller quantities, as trace compounds, within gas emissions from disposal sites. Under the EMEP/EEA (2023) methodology, these emissions are represented as a fixed fraction of CH_4 emissions.

2.3.1. Activity Data

To estimate emissions from solid waste disposal, annual solid-waste series were constructed at the commune level for the domestic and industrial sectors (Table S3.2 and S3.3); the reconstruction of earlier years is required because the First Order Decay model accounts for waste deposited in previous decades. The analysis of emissions focuses on the 2005–2022 period.

A regional per-capita waste generation rate was calculated dividing the total regional waste quantities reported in the INGEI (MMA, 2024a) for the 1950 - 2022 period by corresponding regional population. This rate was multiplied by the commune-level population to obtain annual domestic waste generation for each commune. Population data, at both regional and commune level, were taken from commune level population series (1952-2024) constructed for this study from the 2017 Census and INE intercensal projections (INE, 2017a; Table S3.4). Waste composition was assigned using six material fractions (organic matter, paper/cardboard, plastics, glass, metals, and other; Table S2.5). Only biodegradable fractions were used to estimate CH_4 generation; plastics, glass and metals were excluded.

Final disposal sites and their management types were identified using several SUBDERE datasets (2013, 2018, and 2024), which specify the facility in use and its management system for each

https://doi.org/10.5194/essd-2026-850
Preprint. Discussion started: 13 November 2026
© Author(s) 2026. CC BY 4.0 License.



commune; the references to these databases are provided in the Supplementary Material (Sect. S2; Table S2.1). Management systems were classified into managed and unmanaged sites, where managed sites correspond to sanitary landfills, and unmanaged sites include dumpsites and open dumps. An annual time series of active disposal sites and their management status was constructed for the full study period, assuming the temporal persistence of sites identified as active in 2012 (SUBDERE, 2013) for preceding years, accounting for the reported opening of new facilities or the cessation of operations in others. From this series, the registry of domestic disposal sites, with each site's classification for 2005 and 2022, is reported in the Supplementary Material (Table S3.5). Domestic waste estimates for each commune were then allocated to the corresponding disposal site based on the yearly facility information.

Annual industrial solid waste quantities (Table S3.3) were obtained from the RETC database (MMA, 2024b) for the 2015–2022 period. To extend this series back to 1960, we first reconstructed historical regional GDP as the product of national GDP series (World Bank, 2024) and the annual regional share of economic activity. Regional shares were compiled from the MIDEPLAN regional GDP splicing series (1960-2001; MIDEPLAN, 2004), and Central Bank regional accounts (2013-2022; BCC, 2024), with linear interpolation used to fill the intermediate years (2002-2012) (Table S2.1). Region-specific constant waste generation factors were then derived by dividing total reported industrial waste by regional GDP over the 2015-2022 baseline and applied to the reconstructed regional GDP for the 1960-2014 period. While we acknowledge that more elaborate approaches could be applied to refine these estimates, this methodology represents a necessary first-order approximation. We recognize the limitations of this constant-factor assumption, and its potential impact on our results is explicitly discussed in Section 5; further refinements to this methodology will be considered in future versions of this dataset.

Waste composition in the RETC database is reported using European Waste List (EWL) codes, which were grouped into six biodegradable categories: food, beverages, and tobacco (excluding sludge); pulp and paper; agricultural sludge and pulp residues; wood; textiles; and others. Construction and demolition waste was excluded from this study, as it consists primarily of inert materials with negligible potential for CH_4 generation.

Because facility-level reporting in the RETC is not consistent across years, a list of industrial disposal facilities was compiled by merging all reported facilities and retaining those with consistent presence over time. This registry, with each facility's classification for 2005 and 2022, is listed in the Supplementary Material (Table S3.6). Management types for each site were assigned based on the classifications provided in the RETC records (see Table S2.1). Regional industrial waste quantities were then allocated to the consolidated disposal facilities within each region.

https://doi.org/10.5194/essd-2026-850
Preprint. Discussion started: 13 November 2026
© Author(s) 2026. CC BY 4.0 License.



Tables S3.5 and S3.6 report the full input registries of domestic (207) and industrial (238) disposal sites. During the spatial allocation, domestic and industrial sites whose gridded footprints fall within the same 0.01° cell (that is, co-located within the grid resolution, about 1 km) were merged into a single physical site and their emissions summed, yielding the 331 distinct sites reported in the Results.

2.3.2. Emission Estimation Methods

CH_4 emissions from solid waste disposal were estimated following the First Order Decay (FOD) model recommended in the IPCC Guidelines (2006; 2019), while NMVOC emissions were estimated using the EMEP/EEA (2023) methodology.

The estimation of CH_4 generated first requires quantifying the mass of degradable organic carbon available for decay (DDOCm), calculated as the product of the mass of waste deposited (W), its degradable organic carbon fraction (DOC, i.e. the mass of organic carbon per unit mass of waste that is potentially available for decomposition), the fraction of that carbon that actually decomposes under the anaerobic conditions of the disposal site (DOC_f), and the methane correction factor (MCF). DOC and DOC_f depend on waste composition, whereas MCF reflects the management conditions of the disposal site. Country-specific values for DOC, DOC_f and MCF were derived from INGEI (MMA, 2024a) (Sect. S2; Table S2.3).

$$DDOCm_t = W_t \cdot DOC \cdot DOC_f \cdot MCF \qquad (5)$$

Under the FOD formulation, decomposition follows first-order kinetics, meaning that the rate of degradation depends only on the remaining amount of degradable carbon at the site and on decay rate constant k (yr^{-1}), whose IPCC default values vary with climate and waste type (Sect. S2; Table 2.3). Therefore, emissions in a given year depend not only on the waste deposited in that year but also on the organic carbon accumulated from previous years. In line with the IPCC default modelling assumption, a one-year delay was assumed between waste deposition and the onset of methane generation. This ensures the inter-annual accumulation of degradable organic carbon mass (DDOCm) is accounted for throughout the study period (1960–2022). The mass of degradable organic carbon accumulated in the disposal site at year t ($DDOCma_t$) is estimated as the sum of degradable organic carbon deposited during that year ($DDOCm_t$) and the fraction of the carbon remaining from previous years ($DDOCma_{t-1}$) that persists after decay (e^{-k}), as shown in Eq. (6). The amount of DDOCm decomposed during year t is estimated as the fraction of the accumulated stock from the previous year that decays (Eq. 7).

$$DDOCma_t = DDOCm_t + (DDOCma_{t-1} \cdot e^{-k}) \qquad (6)$$

$$DDOCm\ decomp_t = DDOCma_{t-1} \cdot (1 - e^{-k}) \qquad (7)$$

https://doi.org/10.5194/essd-2026-850
Preprint. Discussion started: 13 November 2026
© Author(s) 2026. CC BY 4.0 License.



This decomposed carbon is then converted into methane assuming that the generated landfill gas is 50 % CH_4 by volume (F=0.5), as shown in Eq. (8), while the remaining fraction is released as CO_2, along with minor amounts of NMVOC. The stoichiometric ratio 16/12 is applied to convert the mass of degraded carbon into CH_4 mass.

$$CH_4 generated_t = DDOCm\ decomp_T \cdot F \cdot 16/12 \qquad (8)$$

Annual CH_4 emissions from each site (x) were calculated by adjusting the total generation for gas recovery (R_t) and oxidation in the site cover (OX_t) as shown in Eq. (9). Recovered methane was reported at regional level by MMA (2024c), obtained through a Transparency Law request (Sect. S3; Table S3.7), and allocated to sanitary-landfills sites in proportion to their share of regional landfill generation. Oxidation followed the IPCC default value (OX_x=0.1 for sanitary landfills; 0 otherwise). A summary of these parameters, including their specific source, is detailed in the Sect. S2 (Table S2.3).

$$SWD_{CH_4} = \left[\sum_x CH_4 generated_{x,t} - R_{x,t}\right] \cdot (1 - OX_x) \qquad (9)$$

Additionally, NMVOC emissions were estimated by multiplying the annual CH_4 emissions from each disposal site by the corresponding default emissions factor. The source of this factor and its specific value are detailed in Sect. S2 (Table S2.2).

2.4. Wastewater Treatment and Discharge

Wastewater treatment and discharge (WWTD) emissions were estimated for domestic and commercial sectors. The industrial sector was excluded from this version due to difficulties in obtaining and processing national data. According to the national inventory, industrial wastewater represents a minor share of wastewater-sector emissions, dominated by domestic sources (MMA, 2024a); its omission is therefore not expected to substantially affect national totals. Industrial wastewater will be incorporated in future updates.

Emissions were estimated per pollutant according to the system and pathway involved. In Chile, wastewater disposal systems were classified into collected (sewer networks) and non-collected (on-site) systems; collected systems may or may not receive treatment before their effluent is discharged to receiving water bodies.

CH_4 was estimated for all system categories, because it is produced under the anaerobic conditions represented by the methane correction factor (MCF) of each system. N_2O was estimated only for collected systems (treated and untreated) through the effluent pathway, i.e., from the nitrogen discharged to aquatic environments (IPCC, 2019). N_2O produced inside treatment plants during nitrification and denitrification was not included, as it is significant only in facilities with

https://doi.org/10.5194/essd-2026-850
Preprint. Discussion started: 13 November 2026
© Author(s) 2026. CC BY 4.0 License.


controlled biological nitrogen removal, which are not representative of Chile; it may be added in future updates. N_2O from non-collected systems was likewise not included in this version, because their effluent infiltrates the soil rather than discharging to receiving waters, and the associated soil N_2O is conventionally reported under agricultural soils (IPCC, 2019). NMVOC was estimated only for collected-treated systems, consistent with the volatilization of dissolved organic compounds during aerated treatment (EMEP/EEA, 2023). No comparable emission factor was available for untreated and on-site systems. NH_3 was estimated only for septic systems, where ammonia volatilizes from the untreated effluent stored on site (EMEP/EEA, 2023). In sewered systems this volatilization is minor, and the nitrogen instead remains in the wastewater and is discharged in the effluent, where it is accounted for through the N_2O pathway.

2.4.1. Activity Data

Two main activity data sources were used, depending on the pollutant and system type: treated wastewater volumes (SISS, 2024b; Table S3.8) and population (INE, 2017a; Table S3.4).

Disposal systems were first classified using fractions derived from the CASEN survey (MDSF, 2024; Sect. S2, Table S2.1), which distinguish sewer-connected (collected) from on-site (non-collected) systems. As CASEN is not conducted annually, these fractions were interpolated and extrapolated over the study period. Computed at the regional level and by urban and rural area, the fractions (Table S3.9) were applied to the commune-level population (INE, 2017a; Table S3.4) to obtain the collected and non-collected population in each commune. Within the collected population, the treated and untreated shares were obtained from SISS sanitary coverage reports (SISS, 2024a; Table S3.10), which give the fraction of collected wastewater that receives treatment in each locality.

For the treated fraction of collected systems, CH_4 and NMVOC emissions were based on the treated wastewater volumes (m^3) reported by the SISS for the 2005–2022 period (SISS, 2024b; Sect. S2, Table S2.1), whereas N_2O was based on the corresponding population. For untreated-collected and non-collected systems, all emissions were based on the commune-level population.

Regarding spatial allocation, emissions from collected systems were assigned to the specific geographic coordinates of the treatment plants reported by SISS. Conversely, emissions from non-collected systems, which occur in both urban and rural areas, were distributed using urban blocks and rural census entities as a spatial proxy, based on INE geodata (INE, 2017b). All data sources, including the SISS, CASEN, and INE population and cartographic data, are detailed in the Supplementary Material (Section S2; Table S2.1).

https://doi.org/10.5194/essd-2026-850
Preprint. Discussion started: 13 November 2026
© Author(s) 2026. CC BY 4.0 License.



2.4.2. Emission Estimation Methods

To estimate CH_4 emissions, the total organic matter available for methane production (TOW) was first calculated based on biochemical oxygen demand (BOD). For collected-treated systems, TOW was derived from the product of wastewater volumes (m^3) and BOD concentrations (kg BOD m^{-3}) reported by SISS. For collected-untreated and non-collected systems, TOW was estimated from commune-level population data and country-specific per-capita BOD values reported in INGEI (Sect. S2; Table S2.3).

CH_4 emissions were then estimated as the fraction of organic matter available for anaerobic degradation after accounting for sludge removal (S), multiplied by the system-specific emission factor (the product of the maximum CH_4 producing capacity B_0 and the methane correction factor MCF) (Eq. 10). These parameters are reported in the Supplementary Material (Sect. S2; Table S2.3). Sludge quantities for collected–treated systems were obtained from SISS records and scaled by a treatment specific removal factor; for collected–untreated systems no sludge removal was assumed (S = 0), while for non-collected systems a sludge fraction of 0.5 was applied only to septic systems and 0 to all other system types (Sect. S2; Table S2.3). Where the estimated sludge removal exceeded the available organic load (S > TOW), CH4 was constrained to zero as a physical lower bound.

$$WWTD\ CH_4 = \left[(TOW_j - S_j) \cdot EF_j\right] \quad (10)$$

N_2O emissions were estimated for collected systems (both treated and untreated) based on the total nitrogen load in collected wastewater (TN). TN was estimated using commune-level population (P), country-specific per-capita protein consumption, the fraction of nitrogen in protein (F_{NPR}), and correction factors accounting for nitrogen from non-consumed protein, industrial and commercial co-discharge, and household products (N_{HH}, $F_{NON\text{-}CON}$, and $F_{IND\text{-}COM}$), as shown in Eq. (11). Per-capita protein consumption and nitrogen content of protein were obtained from INGEI, while default correction factors were applied (Sect. S2; Table S2.3).

$$TN = (P \cdot Protein \cdot F_{NPR} \cdot N_{HH} \cdot F_{NON-CON} \cdot F_{IND-COM}) \quad (11)$$

The nitrogen discharged in the effluent (N) was obtained as the product of the TN and the fraction of nitrogen not removed during treatment (1 - N_{REM}) (Eq. 12). In this version no nitrogen removal was assumed (NREM = 0), so the full nitrogen load is treated as discharged to the effluent.

$$N = \sum_j \left[TN \cdot (1 - N_{REM,j})\right] \quad (12)$$

Finally, annual N_2O emissions were estimated by multiplying the discharged nitrogen (N) by the default emissions factor (kg N_2O-N per kg N discharged) for nitrogen discharged to aquatic

https://doi.org/10.5194/essd-2026-850
Preprint. Discussion started: 13 November 2026
© Author(s) 2026. CC BY 4.0 License.



environments (Sect. S2; Table S2.2) and converting from N_2O-N to N_2O using the molecular weight ratio 44/28 (Eq. 13).

$$WWTD\ N_2O = N \cdot EF \cdot \frac{44}{28} \quad (13)$$

NMVOC emissions were estimated for collected-treated systems using treated wastewater volumes, consistent with their generation through volatilization in aerated treatment processes. Emissions were calculated by multiplying the treated wastewater volumes by the default NMVOC emission factor (Sect. S2; Table S2.2).

NH_3 emissions were estimated only for septic systems (a subset of the non-collected systems), where volatilization of total ammoniacal nitrogen (TAN) occurs. Emissions were calculated by multiplying commune-level population data by the default NH_3 emission factor (Sect. S2; Table S2.2).

2.5. Grid 0.01° x 0.01° distribution

Emissions were spatially allocated using a downscaling approach to the INEMA national grid at 0.01° x 0.01° resolution. For this purpose, activity data were linked to spatial proxies representing either point sources (e.g., treatment plants, disposal sites, livestock establishments) or area sources (e.g., pastureland, urban and rural census units) (Table 3). Area-based sources were distributed proportionally to the share of each proxy overlapping a grid cell, while point sources were assigned directly to the grid cell containing their geographic coordinates. Grazing livestock emissions were distributed over the pastureland within each commune. In communes where livestock were present but no pastureland was mapped (mainly in the altiplano and semi-arid northern zones), these emissions were instead assigned to the commune centroid, ensuring that the full emission mass was conserved during the spatial allocation.

Emissions were initially estimated in tonnes and subsequently converted to gigagrams (Gg) during the gridding process. As a result, emissions are provided as annual totals in Gg on a 0.01° x 0.01° spatial grid.

Table 3: Spatial datasets and territorial units by sector for emission distribution

Spatial source type	Activity source	Spatial unit / proxy	Data/source
Area Source	Grazing livestock production*	Pasture land cover	CR2 LUC (Boisier et al., 2024a)
	Non collected wastewater	Urban blocks and rural census entities	INE, 2017b

https://doi.org/10.5194/essd-2026-850
Preprint. Discussion started: 13 November 2026
© Author(s) 2026. CC BY 4.0 License.



Point Source	Solid waste disposal	Domestic and industrial sites	RETC (MMA, 2024b) SUBDERE, 2013, 2018, 2024
	Collected wastewater	Wastewater treatment plants	SISS, 2024b
	Confined livestock production	Livestock establishment	SAG, 2024

Note. Full data-source details are provided in Sect. S2 (Table S2.1); the spatial allocation of each source is described in the corresponding sector section. *Communes without mapped pastureland were allocated to the commune centroid.

3. Results and discussion

National emissions increased over the study period for all pollutants estimated in this study. CH_4 emissions increased by 37 % between 2005 and 2022, driven primarily by SWD. Meanwhile, N_2O, NMVOC and NH_3 emissions increased by 43 %, 58 %, and 64 %, respectively, mainly due to livestock manure management (Fig. 2). Because these sectors represent distinct socio-economic and biological processes, their contributions and temporal patterns differ, reflecting the internal drivers of each source. A summary of emissions for 2005 and 2022 is presented in Sect. S4; Table S4.1.

Enteric fermentation shifted from the leading CH_4 contributor in 2005 to the second largest in 2022, as its emissions declined while the solid waste disposal sector grew rapidly (rising by 138 %). Livestock manure management was the main contributor to N_2O, NMVOC, and NH_3 emissions, increasing across all three pollutants over the study period. The wastewater sector made comparatively minor contributions to national totals. The current dataset includes only domestic wastewater; industrial wastewater is expected to be relatively small according to the national inventory (MMA, 2024a).

https://doi.org/10.5194/essd-2026-850
Preprint. Discussion started: 13 November 2026
© Author(s) 2026. CC BY 4.0 License.

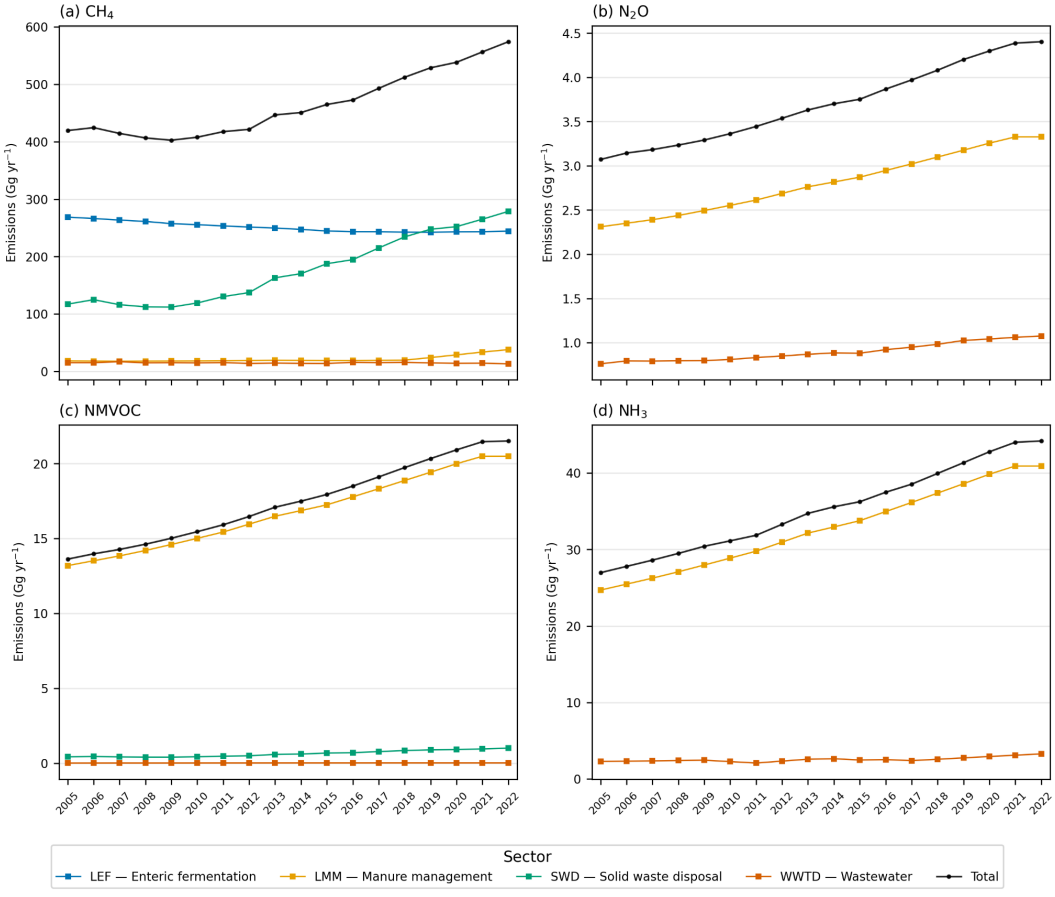


Figure 2. National annual emissions of CH_4, N_2O, NH_3, and NMVOCs in Chile, 2005-2022 (Gg yr^{-1}). Colours denote sectors: SWD (green), LEF (blue), LMM (yellow), and WWTD (purple); the black line is the total.

The livestock sector was a major contributor to national emissions throughout the study period. In 2022, it accounted for 49 % of national CH_4 emissions, predominantly from enteric fermentation, while manure management was the primary national source of NH_3 (93 %), NMVOC (95 %), and N_2O (75 %) that year. Contributions varied markedly across livestock species and management systems (Table 4). Detailed livestock population by species is presented in Section S4; Table S4.2.

The decline in enteric CH_4 emissions, from 268.9 Gg yr^{-1} in 2005 to 244.4 Gg yr^{-1} in 2022 (about 9 %), is explained mainly by a contraction of the non-dairy cattle population, driven by economic pressures (Morales and Martinez, 2025; INE, 2025). Cattle remained the dominant source of LEF throughout the period, accounting for approximately 86 % of the emissions in 2022 (down from

https://doi.org/10.5194/essd-2026-850
Preprint. Discussion started: 13 November 2026
© Author(s) 2026. CC BY 4.0 License.



88 % in 2005), followed by other livestock, predominantly sheep (about 9 %). The decrease was partially compensated by dairy cattle, whose enteric emission rose from 44.4 to 49.5 Gg yr^{-1} as dairy production intensified, while non-dairy cattle emissions fell from 192.0 to 160.2 Gg yr^{-1}.

Conversely, the increase in manure management emissions is driven by the growth of the swine and poultry populations, which together account for the majority of CH_4, N_2O, NH_3, and NMVOC emissions from this source (84 %, 93 %, 92 % and 93 %, respectively, in 2022; Table 4). Within LMM, CH_4 emissions grew over the period, particularly in the last five years, driven almost entirely by swine (swine manure CH_4 rose from 3.7 to 20.7 Gg yr^{-1} between 2005 and 2022). Because manure CH_4 remains a small fraction of national CH_4 emissions, this growth is less apparent in Fig. 2. This trend is directly associated with the adoption of significantly higher country-specific emission factors for swine, as reported by INGEI (MMA, 2024a). Although the underlying drivers are not fully constrained, they likely reflect structural shifts in swine production systems, including modifications in manure management practices and feed intake (Baumberger et al., 2023). The dominance of swine and poultry within LMM reflects the prevalence of high-intensity confined production systems.

Table 4. Emissions from enteric fermentation and manure management by livestock type in 2005 and 2022 (Gg yr^{-1}).

Livestock type	CH_4 (LEF)		CH_4 (LMM)		N_2O (LMM)		NH_3 (LMM)		NMVOC (LMM)	
	2005	**2022**	**2005**	**2022**	**2005**	**2022**	**2005**	**2022**	**2005**	**2022**
Poultry	NA	NA	7.81	11.17	1.75	2.49	10.03	16.25	9.99	15.86
Dairy Cattle	44.36	49.54	3.42	3.25	0.18	0.15	3.06	2.89	1.21	1.12
Other Cattle	192.02	160.17	1.99	1.82	0.06	0.07	0.58	0.6	0.37	0.38
Other livestock	28.02	26.12	1.41	1.1	—	—	—	—	—	—
Swine	4.47	8.57	3.7	20.72	0.32	0.62	11.1	21.3	1.65	3.17
Total	268.87	244.4	18.34	38.06	2.32	3.34	24.77	41.04	13.22	20.53

Note: Poultry do not produce CH_4 from enteric fermentation. N_2O and NH_3 and NMVOC reported for non-dairy cattle correspond exclusively to the fraction of calves managed under confinement; emissions from grazing manure deposition (remaining non-dairy cattle and other livestock) are excluded here and will be reported under agricultural soils in future INEMA updates. NA: no applied

While CH_4 emissions from grazing are included (Table 4), the current estimates exclude NH_3, N_2O and NMVOC emissions from manure deposited on pasture. N_2O from grazing is conventionally reported under agricultural soils (IPCC, 2019). The exclusion of grazing-related NH_3 and NMVOC means that the relative contribution of swine and poultry may be overrepresented within the

https://doi.org/10.5194/essd-2026-850
Preprint. Discussion started: 13 November 2026
© Author(s) 2026. CC BY 4.0 License.



agricultural sector (Castesana et al., 2018; MMA, 2024a). These grazing-related emissions are planned for inclusion in future updates of the INEMA inventory.

The SWD sector showed the largest relative increase in CH_4 emissions of all sectors (Fig. 2), rising by 138 % between 2005 and 2022. Its shares of national CH_4 increased from 28 % to 49 %, marking it the dominant national CH_4 source. This growth is driven primarily by a 68 % increase in the volume of biodegradable waste sent to final disposal, with domestic waste consistently the largest fraction. Because emissions grew faster than the waste volume, the trend also reflects evolving management practices; the share of waste disposed in sanitary landfills rose from 59 % in 2005 to 87 % in 2022. Although this transition improved environmental control, it promoted more anaerobic conditions that unintentionally increase methane generation potential (IPCC, 2019; Bogner and Matthews, 2003). A temporary decrease in CH_4 emissions in 2006-2010 (Fig. 3), coincided with a period of increased methane recovery.

SWD also contributes to NMVOC emissions, which increased from 0.42 Gg yr^{-1} in 2005 to 1.0 Gg yr^{-1} in 2022, about 5 % of national NMVOC emissions that year.

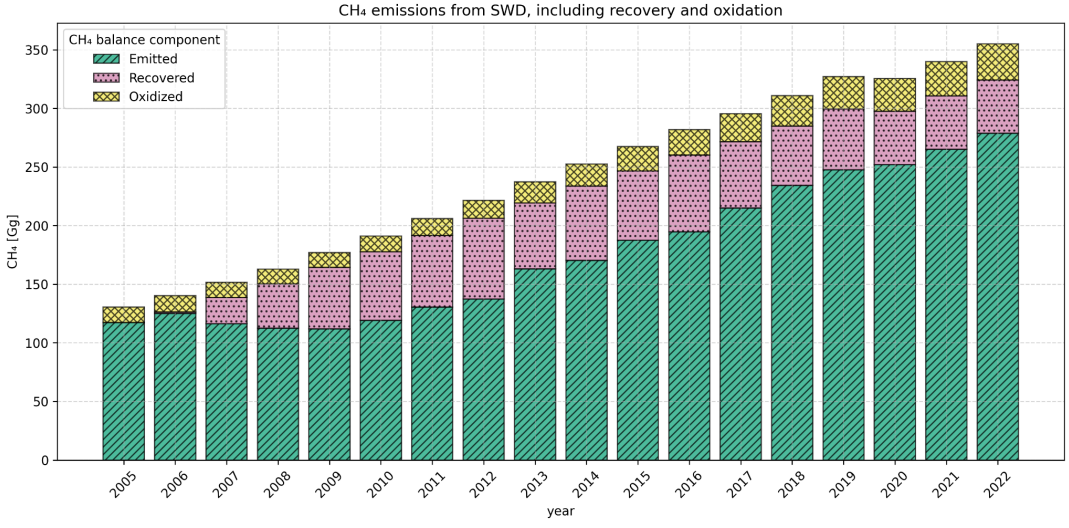


Figure 3: Methane mass balance in Chile's solid waste disposal sector, 2005-2022. Bars partitions total generated CH_4 into oxidized (yellow), recovered (pink), and emitted (green) methane (Gg yr^{-1}).

WWTD represented a relatively minor contribution to total national emissions (Fig. 2). However, it is a significant source of N_2O, accounting for approximately 25 % of the national total in both 2005 and 2022 (Sect. S4; Table S4.1). Within the wastewater sector, CH_4 emissions remained

https://doi.org/10.5194/essd-2026-850
Preprint. Discussion started: 13 November 2026
© Author(s) 2026. CC BY 4.0 License.



relatively stable, with a slight overall decline over the period despite population growth and rising wastewater generation, reflecting two opposing dynamics (Table 5). Emissions from collected systems increased with population growth and expanding sewer coverage, particularly in urban areas, but remained comparatively low because part of the organic load is removed as sludge before anaerobic degradation. Emissions from non-collected, by contrast, decreased overall and drove the net decline. Septic-system emissions rose as their coverage expanded, although sludge removal limiting CH_4 generation. Latrine emissions, which have no sludge removal and therefore emit more per unit of organic load, decreased substantially. This drop in latrine emissions outweighed the septic-system and collected-system increases, producing the net downward trend.

Finally, in a limited number of collected–treated cases, the independent reporting of treated volumes, BOD and sludge by SISS caused the estimated sludge removal to exceed the available organic load (S > TOW), producing negative CH4 values; these were constrained to zero, increasing the collected–treated CH4 total by about 2 %.

NH_3 emissions were estimated exclusively for septic systems (a non-collected category). As the population served by septic systems increased, wastewater NH_3 emissions also rose by 43 % over the period (Table 5). NMVOC was estimated only for collected-treated systems, whereas N_2O was estimated for collected systems (treated and untreated) via the effluent pathway. Both increased over time (Table 5), consistent with population growth, expanded sewer coverage and increasing volumes of treated wastewater.

Table 5: Pollutant emissions from collected and non-collected wastewater systems in 2005 and 2022 (Gg yr⁻¹).

System	CH_4		N_2O		NMVOC		NH_3	
	2005	2022	2005	2022	2005	2022	2005	2022
Collected	5.40	6.52	0.8	1.13	0.01	0.02	—	—
Non collected	9.88	6.72	—	—	—	—	2.29	3.28
Total	15.28	13.24	0.8	1.13	0.01	0.02	2.29	3.28

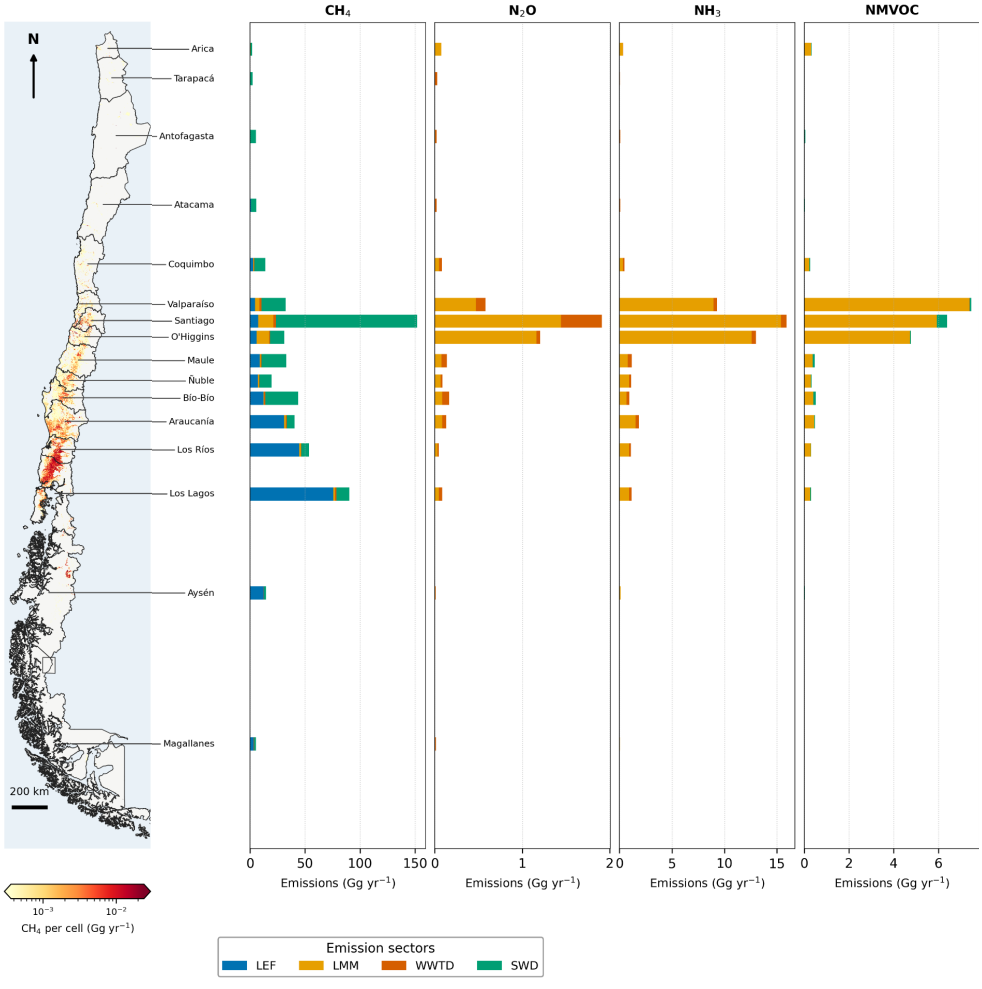
Regarding spatial distribution, in 2022 emissions of all evaluated pollutants were markedly concentrated in the central and southern zones of the country in (Fig 4). The spatial pattern of CH_4 emissions illustrates this heterogeneity, with diffuse livestock sources in the south. SWD emissions are highly localized in the central zone, particularly within the Santiago Metropolitan Region, which hosts about 40 % of the national population; as these are point sources concentrated in a few grid cells, this SWD dominance is most evident in the regional bars (Fig. 4). In contrast, LEF emissions dominate the southern zone as diffuse area sources across regions with extensive pasture-based cattle systems.

https://doi.org/10.5194/essd-2026-850
Preprint. Discussion started: 13 November 2026
© Author(s) 2026. CC BY 4.0 License.



Open Access Earth System Science Data Discussions

607 Other pollutants follow similar socio-economic and geographic drivers. The central zone
608 concentrates large-scale, high-intensity confined swine and poultry production facilities; these
609 specific agricultural clusters account for the vast majority of national agricultural N_2O and NH_3
610 emissions within the LMM sector (Fig. 4). In contrast, the northern and austral zones contributed
611 only marginally to national emissions of all evaluated pollutants, consistent with their low
612 population density and limited agricultural and waste-sector activity.



613
614 *Figure 4: Emissions in 2022. Left: total CH_4 per 0.01° grid cell (Gg yr^{-1}, log scale); SWD point*
615 *sources appear as small high-intensity cells but are quantified in the bars. Right: per-region*
616 *stacked emissions of CH_4, N_2O, NH_3 and NMVOC by sector; note the different horizontal-axis*
617 *scales.*

https://doi.org/10.5194/essd-2026-850
Preprint. Discussion started: 13 November 2026
© Author(s) 2026. CC BY 4.0 License.



These patterns are consistent with national sectoral trends observed over time. By incorporating precisely these sectors, the previous high-resolution inventory for Chile (Álamos et al., 2022) is complemented, providing a spatially explicit picture of how these pollutants, and methane in particular, are distributed across the country. Sectors still outside the present scope, such as agricultural soils, may also contribute and could modify the relative sectoral balance; their integration is planned for future versions of INEMA. A notable exception occurs for NMVOC: residential wood burning for heating is an important source of NMVOC in southern Chile (Álamos et al., 2022), so its inclusion would markedly increase NMVOC in the southern zone and shift the relative importance of the waste and livestock sectors for this pollutant, likely yielding a more balanced distribution between the central and southern zones.

At finer scale, Fig. 5 zooms into the central zone and maps the leading emission sector within each 0.01° grid cell, revealing a fine-grained mosaic in which landfill point sources (SWD) appear as discrete hotspots and livestock dominates the rural cells. Wastewater (WWTD) is the leading sector in a large number of cells; this reflects that it is the most spatially ubiquitous source, following population across the inhabited valleys, rather than the largest in absolute terms (nationally, WWTD is the smallest CH_4 source; see Fig. 2 and Table 5). The equivalent maps for N_2O, NH_3 and NMVOC are provided in Sect. S4; Fig. S4.1.

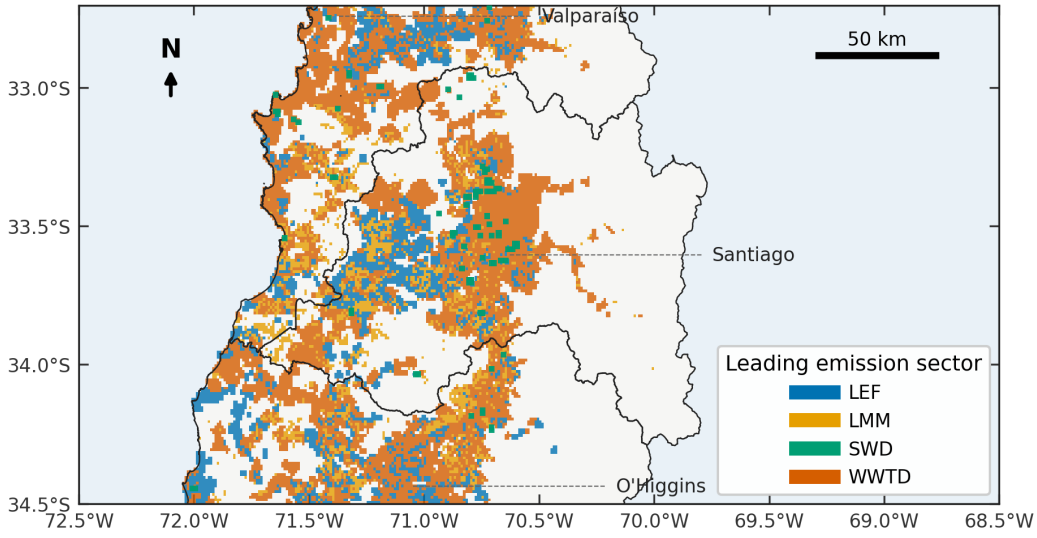


Figure 5: Leading emission sector for CH_4 per 0.01° grid cell over central Chile (Valparaíso, Metropolitan, O'Higgins), 2022. Colour shows the highest-emitting sector per cell, not its magnitude; WWTD leads widely only because it is the most spatially ubiquitous (population-driven) source. SWD point sources appear as green cells.

https://doi.org/10.5194/essd-2026-850
Preprint. Discussion started: 13 November 2026
© Author(s) 2026. CC BY 4.0 License.



4. Comparison and Assessment of Inventory Robustness

4.1. Comparison with other inventories

Emissions of CH_4, N_2O, NH_3 and NMVOC for the period 2005-2022 were compared with the National GHG inventory INGEI (MMA, 2024a) and the global gridded product EDGAR (V.8; Crippa et al., 2024). The temporal evolution and sectoral contributions of these pollutants are illustrated in Fig. 6.

Although INEMA and the official INGEI share several underlying national activity datasets, their critical distinction lies in spatial resolution: while INGEI aggregates data at a coarse regional level, INEMA delivers a high-resolution 0.01° x 0.01° grid specifically tailored for atmospheric modeling. Furthermore, discrepancies between these national datasets stem from updated emission factors and distinct sectoral scopes, whereas deviations from EDGAR are primarily driven by its reliance on global top-down statistical downscaling and generalized emission factors that consistently fail to capture local operational realities.

Regarding specific pollutants, EDGAR reported higher absolute CH_4 emissions than both national datasets while exhibiting a contrasting temporal behavior; whereas EDGAR showed near-stable emissions over the period, the national inventories displayed a sustained upward trend toward 2022. This divergence is largely explained by differences in sectoral attribution, as EDGAR assigns a substantially larger share of CH_4 emissions to WWTD and a much smaller contribution to SWD, which constitutes the dominant source in national datasets, thereby leading to a distinct structural configuration of national methane emissions.

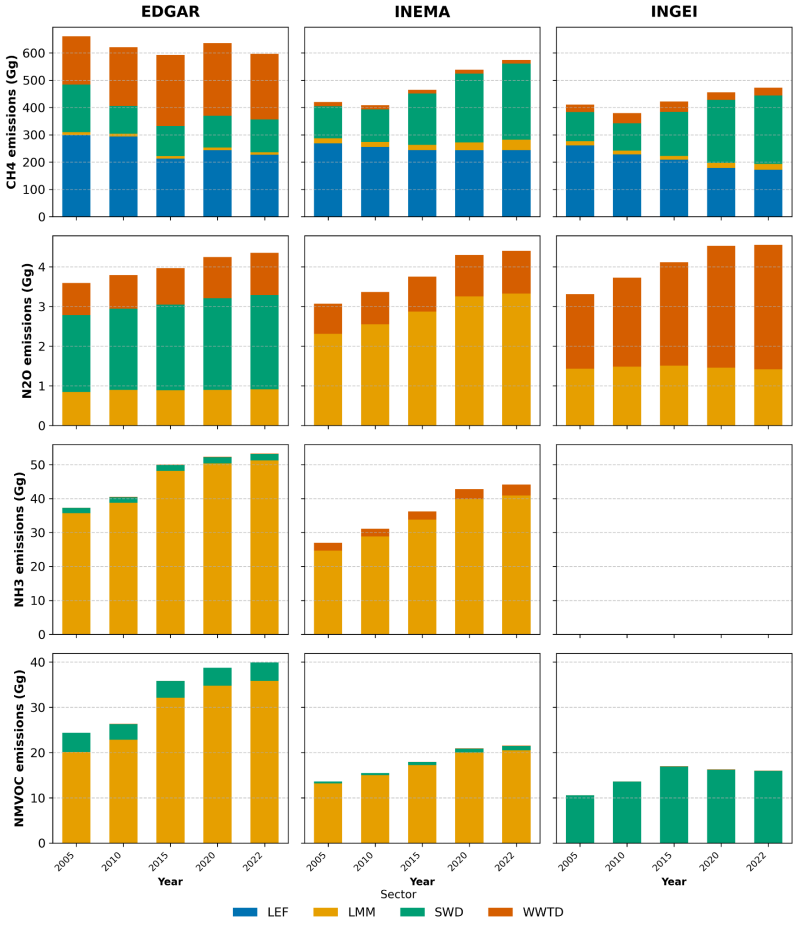
For N_2O, emissions increased over time across all inventories, although national estimates showed stronger growth than EDGAR. Sectoral configurations differed markedly, as EDGAR attributed a large share of N_2O to SWD (a sector excluded from national N_2O inventories due to methodological tier approaches applied) while INEMA and INGEI identified LMM and WWTD as the dominant sources. Notable differences also arose between the two national datasets, where INEMA attributed the majority of N_2O emissions to LMM, driving the observed historical increase, whereas INGEI reported stable LMM emissions and identified WWTD as the primary contributor.

In the case of NH_3, emissions exhibited increasing trends in both EDGAR and INEMA, with EDGAR consistently overestimating the total magnitude; while both identify LMM as the primary source, EDGAR includes emissions from SWD, whereas INEMA accounts for contributions from WWTD, and INGEI completely excludes NH_3 due to its strict focus on greenhouse gases.

https://doi.org/10.5194/essd-2026-850
Preprint. Discussion started: 13 November 2026
© Author(s) 2026. CC BY 4.0 License.



672 Finally, NMVOC emissions displayed the largest discrepancies among the three datasets, where
673 INGEI showed a contrasting temporal trajectory, peaking mid-period and declining recently,
674 EDGAR and INEMA displayed sustained upward trends. EDGAR reported consistently higher
675 NMVOC magnitudes and, alongside INEMA, identified LMM as the principal contributor,
676 whereas INGEI excluded this sector and attributed most NMVOC emissions to SWD, resulting in
677 a considerably higher estimate from that specific source.



678
679 *Figure 6. Comparison of temporal emission trends and sectoral contributions for CH_4, N_2O, NH_3,*
680 *and NMVOCs across the INEMA, INGEI, and EDGAR inventories from 2005 to 2022, highlighting*
681 *differences in magnitude and sectoral structure among datasets.*

682 Overall, differences in emission magnitudes, trends, and sectoral contributions reflect
683 methodological contrasts across inventories. While national inventories rely on country-specific

https://doi.org/10.5194/essd-2026-850
Preprint. Discussion started: 13 November 2026
© Author(s) 2026. CC BY 4.0 License.



684 information, discrepancies remain due to differences in livestock activity data and waste-sector
685 methodologies. In contrast, EDGAR is based on global datasets and generalized assumptions that
686 do not fully capture national circumstances, leading to systematic biases in both emission levels
687 and sectoral attribution. These limitations underscore the importance of national products such as
688 INEMA, which better represent country-specific activity patterns, management practices, and
689 technological conditions.

690 Complementing the temporal and sectoral analyses, the spatial distribution of emissions was also
691 assessed through a comparison of gridded EDGAR and INEMA products. Figure 7 compares the
692 spatial distribution of CH_4 emissions from INEMA and EDGAR over the central zone, placing the
693 two gridded products side by side. In addition to the substantial differences in emission
694 magnitudes, clear contrasts were observed in the spatial allocation of emissions. The EDGAR
695 inventory distributed CH_4 emissions broadly across the national territory, with higher values over
696 urbanized areas and pronounced hotspots in the Metropolitan Region. In contrast, INEMA showed
697 a more spatially focused distribution, with emissions concentrated in pasture dominated areas
698 associated with livestock enteric fermentation and in discrete point sources related to solid waste
699 disposal sites (Fig. 7).

700 These differences reflect the distinct spatial proxies and methodological approaches used by each
701 inventory. EDGAR allocates emissions to grid cells using generalized spatial proxies, including
702 population density, human settlement maps, and other broad indicators of activity to distribute
703 national totals across space (Crippa et al., 2024), which can result in more diffuse spatial patterns
704 and an apparent urban bias in some sectors. In contrast, INEMA explicitly incorporates the
705 geographic location of major point sources and livestock activity, allowing for a more realistic
706 representation of emission sources and spatial heterogeneity.

https://doi.org/10.5194/essd-2026-850
Preprint. Discussion started: 13 November 2026
© Author(s) 2026. CC BY 4.0 License.

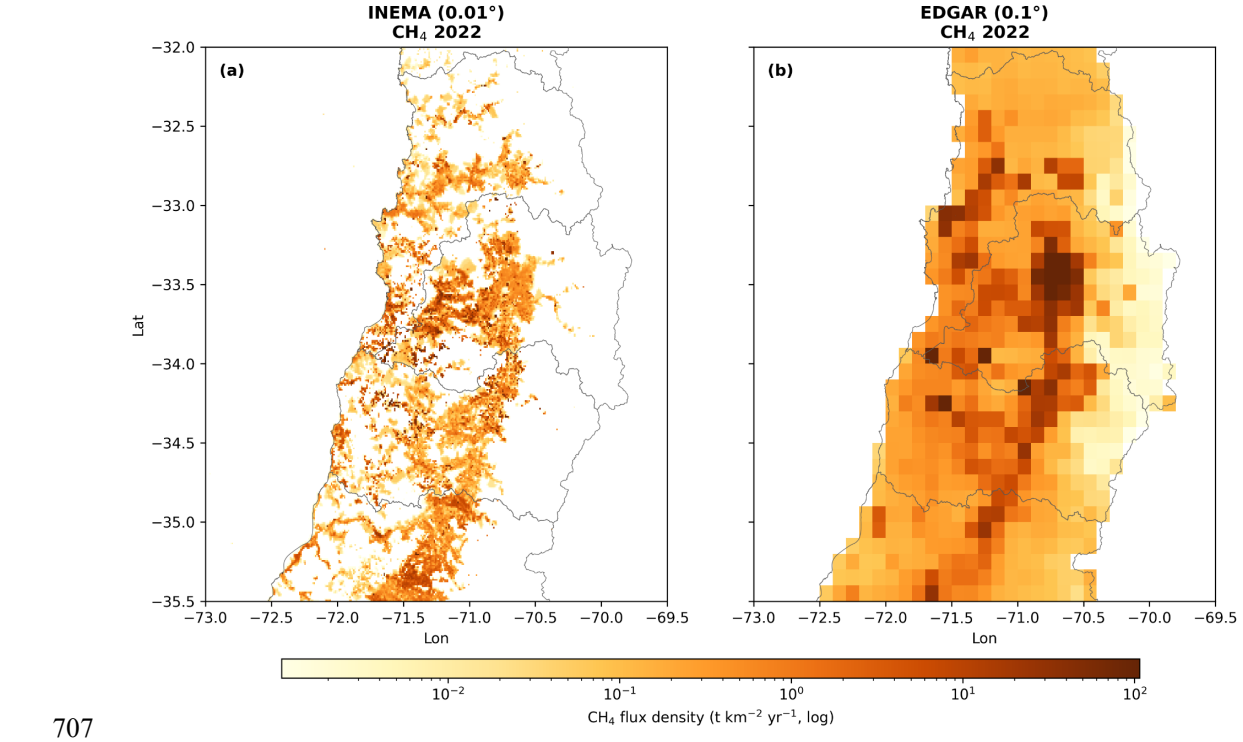


Figure 7. Spatial distribution of CH_4 emissions in central Chile for 2022, expressed as flux density (t km⁻² yr⁻¹, log scale). ***(a)*** *High-resolution INEMA inventory (0.01°);* ***(b)*** *EDGAR v8.0 inventory at its native 0.1° resolution. Both panels share the same colour scale.*

Similar differences in spatial allocation between EDGAR and INEMA were observed for N_2O, NH_3, and NMVOC, although the dominant source regions varied by pollutant. The equivalent map comparisons for these species are provided in Sect. S4; Fig. S4.2.

These contrasts highlight the limitations of global gridded inventories for representing national-scale emission patterns and underscore the importance of country-specific datasets such as INEMA for spatially explicit analyses and the development of targeted mitigation policies.

4.2. Comparison with top-down estimates

Recent advances in imaging spectroscopy enable the direct detection and quantification of individual CH_4 plumes from large point sources, providing independent measurements-based information that complements bottom-up inventories (Petrescu et al., 2024). Here, INEMA was compared against CH_4 plume retrievals from the Carbon Mapper platform (Carbon Mapper, 2025;

https://doi.org/10.5194/essd-2026-850
Preprint. Discussion started: 13 November 2026
© Author(s) 2026. CC BY 4.0 License.



data.carbonmapper.org), which integrates spaceborne and airborne observations from NASA and the airborne AVIRIS-NG spectrometer, all resolving plumes at approximately 30m spatial resolution. Because these sensors detect concentrated point sources rather than diffuse emissions, the comparison was restricted to the solid waste disposal (SWD) sector; diffuse sources such as livestock enteric fermentation cannot be retrieved with this approach and were therefore excluded.

Over the 2023-2025 period, Carbon Mapper detected 184 CH_4 plumes at 16 landfill sites across central and southern Chile (1-20 plumes per site; median 14). Individual plume fluxes (instantaneous emission rates, in kg h^{-1}) were grouped into sites by spatial clustering using 10 km search radius and averaged to obtain a representative top-down flux per site, with the standard deviation across plumes taken as a measure of observational variability. For each site, the corresponding INEMA estimate was obtained by summing the annual SWD CH_4 emissions of all 0.01° grid cells falling within a 10 km buffer around the site and expressing them as an equivalent hourly rate, so that the bottom-up annual average flux and the top-down plume based flux could be compared on common ground (Fig. 8a). The agreement between both estimators was then evaluated on site-by-site bases (Fig. 8b). A 10 km buffer was adopted as a conservative margin that absorbs the offset between the plume-detection centroid and the gridded facility location, while remaining well below the minimum separation between sites (14.6 km); results were insensitive to this radius over the 3–10 km range.

At the national scale, after merging co-located domestic and industrial sites (those sharing a 0.01° grid cell) and summing their emissions, INEMA resolves 331 distinct SWD facilities (compiled from the registries in Tables S3.5 and S3.6); yet emissions are highly concentrated, with just 16 sites accounting for approximately 80 % of the sector's CH_4. All 16 landfills detected by Carbon Mapper correspond to high emitting facilities represented in INEMA, indicating full spatial coincidence between the detected plumes and the largest SWD sources in the inventory (Fig. 8a). Conversely, several high-emissions INEMA sites were not detected by Carbon Mapper, consistent with gaps in airborne flight coverage and satellite revisit frequency, and with the detection sensitivity of these instruments (limited to sources emitting on the order of ~100 kg h^{-1} or more), rather than with differences in emissions magnitude. Across the 16 colocated sites, the two independent estimates are strongly and significantly correlated (Spearman $\rho = 0.87$; Pearson $r = 0.80$ in log space) and all of them agree within one order of magnitude (88 % within a factor of three; Fig. 8b). Carbon Mapper fluxes are on average ~1.5 times higher than INEMA (median 1.4), although the summed emissions across the 16 sites differ by only 17 %. This overestimation is most pronounced at the smaller sites and disappears at the largest landfills, where the INEMA annual estimate matches or slightly exceeds the plume-based value (e.g. Loma Los Colorados, the country's main landfill).

https://doi.org/10.5194/essd-2026-850
Preprint. Discussion started: 13 November 2026
© Author(s) 2026. CC BY 4.0 License.

Open Access Earth System Science Data Discussions

These patterns are physically expected. Carbon Mapper retrievals capture episodic, near-instantaneous plumes preferentially sampled under high-emitting conditions and favourable observing geometries, whereas INEMA reports annual-average, bottom-up fluxes for 2022; a moderate positive bias of the top-down values relative to the annual mean is therefore anticipated, particularly at smaller sites where a few high-emission overpasses dominate the average. At the largest landfills, where sustained high activity is better captured by both approaches, the two estimates converge. The comparison therefore primarily assesses spatial consistency and source relevance rather than exact temporal agreement, and the strong overlap between datasets confirms that a small number of high-emitting waste facilities dominate the sector and constitute priority targets for mitigation. More broadly, it illustrates the complementary value of top-down observations for supporting, evaluating, and progressively refining national bottom-up inventories such as INEMA.

This consistency points to a clear opportunity for coordinated bottom-up/top-down work: national inventories such as INEMA can supply georeferenced priority targets, like the high-emitting landfills identified here, to guide targeted airborne and satellite campaigns, while the resulting plume-level measurements feed back into the inventory as independent constraints to verify and refine facility-level estimates.

https://doi.org/10.5194/essd-2026-850
Preprint. Discussion started: 13 November 2026
© Author(s) 2026. CC BY 4.0 License.

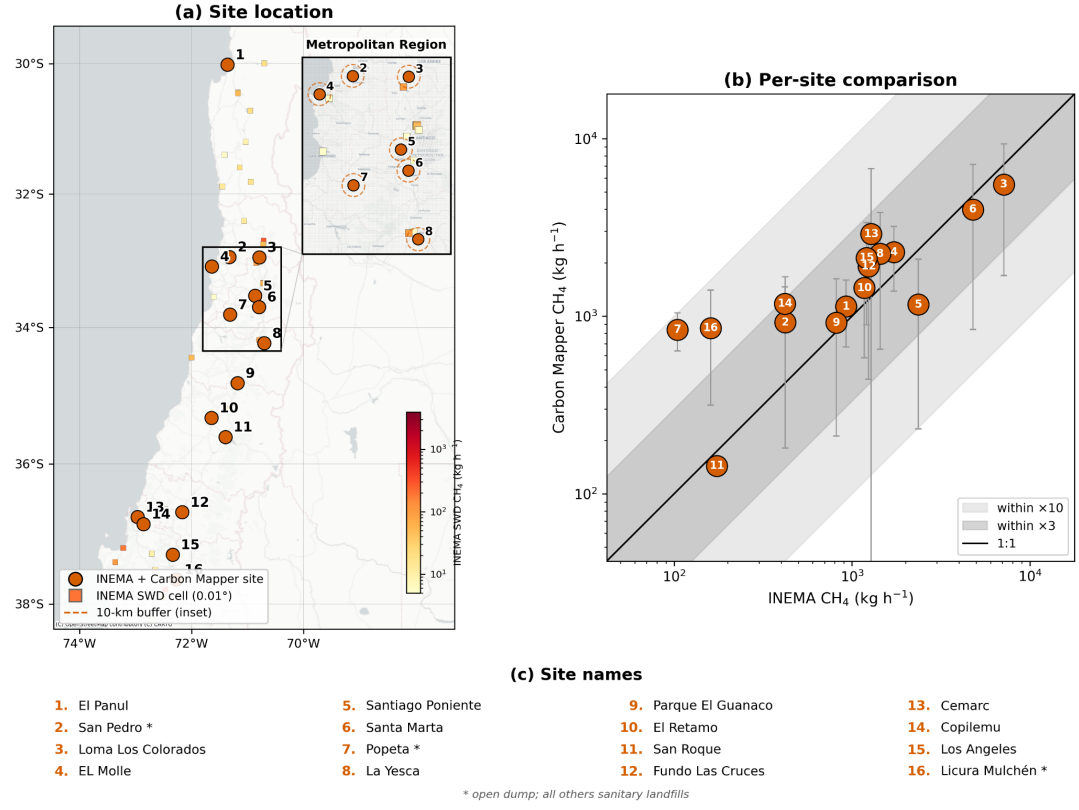


Figure 8. SWD sector CH_4: INEMA bottom-up inventory (2022) versus Carbon Mapper plume observations at 16 co-located landfills. (a) Site location; orange circles, sites detected by both datasets; squares, INEMA SWD grid cells (0.01°) coloured by CH_4 emission; the inset zooms into the Metropolitan Region, with dashed circles showing the 10-km buffer used to match cells to each Carbon Mapper site. (b) Per-site annualized CH_4 fluxes (log–log): 1:1 line, factor-3 and factor-10 agreement bands, and error bars (standard deviation across plume observations). (c) Site names (open dump; others sanitary landfills). Basemap in panel (a): © OpenStreetMap contributors, © CARTO (https://carto.com/attributions).*

5. Progress, considerations, and next steps

The updated INEMA emission inventory represents a substantial advance over previous national assessments by extending its sectoral coverage to include spatially explicit emissions from the livestock and waste sectors. This enhancement enables a more comprehensive characterization of national emissions of CH_4, N_2O, NH_3, and NMVOC. By combining national activity data,

https://doi.org/10.5194/essd-2026-850
Preprint. Discussion started: 13 November 2026
© Author(s) 2026. CC BY 4.0 License.


georeferenced point sources, and sector-specific information, INEMA captures local conditions and production practices that are not adequately represented in global inventories, which typically rely on generalized proxies and harmonized datasets. In this sense, INEMA not only complements global products but also advances existing national datasets by providing high-resolution spatial information and by including air pollutants relevant for air quality and integrated assessment studies.

The spatially explicit structure of INEMA allows for the identification of key emission drivers and distinct spatial patterns across sectors. In particular, it enables differentiation between spatially diffuse processes, such as enteric fermentation in livestock systems, and highly concentrated emissions associated with a limited number of point sources, especially within the waste sector. This level of detail enhances the inventory's usefulness for the design of targeted mitigation strategies and supports territorial planning and policy development at regional and local scales.

Despite these advances, several limitations remain. Some relevant emission sources are not yet included, notably agricultural soils and industrial wastewater, which may influence the interpretation of sectoral contributions, particularly for N_2O and NH_3. In addition, data gaps persist in certain subsectors, leading to partial reliance on default emission factors and an incomplete representation of small-scale or informal activities. For collected–treated systems, treated volumes, BOD and sludge are reported independently by SISS, which in some cases yields inconsistent sludge-to-load ratios. These constraints highlight areas where further data collection and methodological refinement are required.

The emissions estimates also carry uncertainties that differ by pollutant and sector and no formal error analysis specific to INEMA was performed. Because INEMA inherits the emissions factors, methods and much of the activity data from the INGEI, the uncertainties reported by MMA (2024a) provide a valid reference for the magnitude of uncertainty in our estimates. As a reference, Chile's national inventory reports a combined (Approach 1) uncertainty of -43.6 % / + 43.8 % for the national greenhouse-gas balance, with the waste sector among the largest contributors (MMA, 2024a). For livestock, activity data (animal population from agricultural censuses and surveys) carry uncertainties of roughly 10 % to 40 % depending on the data source and gap-filling technique, and methane emission factors are comparatively well constrained for cattle (country-specific, Tier 2) while relying on IPCC defaults for the remaining species (MMA, 2024a; IPCC, 2019). Nitrous oxide carries by far the largest uncertainty: for the domestic wastewater, the INGEI reports a combined N_2O uncertainty of about 139 % to 1539 %, reflecting the very wide range of the effluents emission factor, whereas the corresponding CH_4 uncertainty is close to 70 % (MMA, 2024a). For solid waste disposal, the combined CH_4 uncertainty is on the order of 100 %, dominated by the first order deecy parameters (DOC, DOC_f, MCF, k) and by activity data on the amount and composition of disposed waste (MMA, 2024a). Ammonia and NMVOC, estimated

https://doi.org/10.5194/essd-2026-850
Preprint. Discussion started: 13 November 2026
© Author(s) 2026. CC BY 4.0 License.



with EMEP/EEA Tier 1 factors, are uncertain by roughly a factor of two (EMEP/EEA, 2023). Activity data derived from national census and administrative statistics are comparatively robust, although the spatial disaggregation to establishment locations and pasture areas adds uncertainty to the gridded fields. A formal quantitative (Monte Carlo) uncertainty propagation was not performed and is planned for a future INEMA release.

Looking forward, the progressive integration of satellite and airborne based observations represents a promising pathway to further strengthen INEMA. Such data can improve the spatial characterization of emissions, help identify high-emitting sources, and provide independent information to support the refinement and evaluation of bottom-up estimates. Future developments of INEMA will therefore focus on expanding sectoral coverage, strengthening coordination with national institutions, and increasing the use of country-specific emission factors, with the aim of further enhancing the robustness, transparency, and policy relevance of the inventory.

6. Conclusions

Overall, CH_4, N_2O, NH_3, and NMVOC emissions from livestock and waste sectors were estimated at a spatial resolution of 0.01° x 0.01°, expanding the national emission inventory INEMA and delivering a substantially more complete representation of non-energy emissions in Chile and their evolution over the 2005–2022 period.

The high-resolution estimates show that livestock and waste related activities play a central role in national non-energy emissions. For CH_4, solid waste disposal and livestock enteric fermentation emerge as the dominant contributors at the national scale, while livestock manure management accounts for the largest shares of N_2O and NH_3 emissions and represents a major source of NMVOC emissions. Between 2005 and 2022, emissions of all analyzed pollutants increased markedly, with CH_4 rising by 37 % and N_2O, NH_3, and NMVOC increasing by 43 %, 64 %, and 58 %, respectively. These trends are consistent with changes in underlying activity drivers, including population growth, structural changes in livestock production systems, and increases in waste generation and management.

Beyond national totals, the spatially explicit representation provided by INEMA reveals a combination of spatially diffuse sources, such as pasture-based livestock systems, and a strong concentration of emissions in a limited number of high-emitting facilities, particularly for methane from solid waste disposal. This spatial heterogeneity highlights clear opportunities for targeted and potentially cost-effective mitigation strategies.

Comparisons with the national greenhouse gas inventory (INGEI) show general consistency in emission magnitudes and temporal trends. Differences in sectoral contributions arise primarily

https://doi.org/10.5194/essd-2026-850
Preprint. Discussion started: 13 November 2026
© Author(s) 2026. CC BY 4.0 License.


from methodological choices, emission factors, and the spatial resolution of the inventories. While INGEI reports emissions at the level of administrative regions, the higher spatial resolution of INEMA allows emissions to be attributed to specific locations, providing additional insight into the geographic distribution of emissions. In contrast, discrepancies with the EDGAR inventory underline the limitations of global products based on generalized assumptions and emphasize the value of nationally grounded datasets. The strong spatial coincidence between high-emitting sources identified in INEMA and independent top-down observations from the Carbon Mapper platform further supports the reliability of the inventory, particularly for major point sources.

Overall, this updated version of INEMA constitutes an evolving and policy-relevant tool for national reporting, atmospheric modeling, and mitigation planning. By improving the spatial representation of major emission sources and extending coverage to key pollutants beyond greenhouse gases, it strengthens the evidence base required to design effective climate and air quality strategies at national, regional, and local scales.

Data Availability

The complete INEMA v3.0 gridded dataset for Chile is freely available on Zenodo at https://doi.org/10.5281/zenodo.23169719 (Álamos Correa et al., 2026) under a CC BY 4.0 license. This version integrates the previously published sectors with the livestock and waste sectors (2005–2022) described in this paper. The data are provided as one compressed file per year, each containing one NetCDF (.nc) file per pollutant on a 0.01° × 0.01° grid, with one variable per emission sector expressed as annual mean flux (kg m^{-2} s^{-1}) and a grid-cell area variable to derive annual totals. The sectors described in this paper correspond to the variables agl (livestock enteric fermentation and manure management combined), swd (solid waste disposal) and wwtd (wastewater treatment and discharge).

The publicly available input datasets used to derive these emissions, together with their direct access links and access dates, are listed in Table S2.1 of the Supplement and cited in the reference list. Administrative datasets that are not publicly distributed (livestock establishment records, SAG; operational wastewater data, SISS; and landfill methane recovery data, MMA; all obtained through Chilean Transparency Law and institutional requests) are provided in the Supplement (Sect. S3) as summary tables and site- and plant-level listings, excluding their exact geographic coordinates. Third party datasets used for comparison and evaluation are available from their respective providers: the EDGAR v8.0 global inventory (Crippa et al., 2024; https://edgar.jrc.ec.europa.eu), the national greenhouse-gas inventory INGEI (MMA, 2024a), and CH_4 plume retrievals from the Carbon Mapper platform (Carbon Mapper, 2025; https://data.carbonmapper.org, last accessed 15 September 2025).

https://doi.org/10.5194/essd-2026-850
Preprint. Discussion started: 13 November 2026
© Author(s) 2026. CC BY 4.0 License.



Author contributions

Diana Rojas (DR) and Nicolás Álamos (NA) contributed to the conceptualization of the study, methodology development, data search and preparation, data curation, formal analysis, and investigation. Nicolás Huneeus (NH) contributed to the conceptualization and methodological design of the study, formal analysis, funding acquisition, and supervision. Mariel Opazo (MO) and Ignacio Leiva (IL) contributed to the conceptualization and formal analysis. MO additionally contributed to the design and implementation of gridding codes. Juan Pablo Boisier (JPB), Kevin Basoa (KB) and Ignacio Beltrán (IB) provided activity datasets related to waste and livestock sectors. Tia Scarpelli (TS) contributed to the interpretation of the top-down (Carbon Mapper) plume data and to the review and editing of the manuscript. Mauricio Osses (MaO) reviewed the manuscript and provided transport-sector data that, although outside the scope of this study, supported the interpretation of the results. All authors reviewed the final manuscript.

Competing interests

The authors declare that they have no competing interests.

Acknowledgments

The authors thank the Center for Climate and Resilience Research (CR2) for institutional support. Powered@NLHPC: this research was partially supported by the supercomputing infrastructure of the National Laboratory for High-Performance Computing, Chile (NLHPC, ECM-02), which enabled the computational processing required for this study. During the preparation of this manuscript, the authors used an AI-based assistant (Anthropic's Claude) to help draft and refine portions of the text; the authors reviewed and edited all content and take full responsibility for the final manuscript.

Financial support

This research has been supported by FONDECYT Regular Project No. 1231717, FONDECYT Regular No.1241477, and FONDEF Project ID23I10219.

References

Álamos, N., Huneeus, N., Opazo, M., Osses, M., Puja, S., Pantoja, N., Denier Van Der Gon, H., Schueftan, A., Reyes, R., and Calvo, R.: High-resolution inventory of atmospheric emissions from

https://doi.org/10.5194/essd-2026-850
Preprint. Discussion started: 13 November 2026
© Author(s) 2026. CC BY 4.0 License.



920 transport, industrial, energy, mining and residential activities in Chile. ESSD, 14(1), 361–379,
921 https://doi.org/10.5194/essd-14-361-2022, 2022.

922 Álamos Correa, N., Huneeus, N., Osses, M., Opazo, M., Rojas, D., Bevilacqua, D., and Daswani,
923 K.: INEMA: High resolution inventory of atmospheric emissions of Chile (v3), Zenodo [data set],
924 https://doi.org/10.5281/zenodo.23169719, 2026.

925 Banco Central de Chile (BCC): Statistics Database (BDE): National accounts - gross domestic
926 product (GDP), https://si3.bcentral.cl/siete/en/, last access: 12 September 2025, 2024.

927 Baumberger, C., Di Pillo, F., Galdames, P., Oyarzun, C., Marambio, V., Jimenez-Bluhm, P., &
928 Hamilton-West, C.: Swine backyard production systems in central Chile: Characterizing farm
929 structure, animal management, and production value chain. Animals, 13(12), 2000,
930 https://doi.org/10.3390/ani13122000, 2023.

931 Bogner, J., and Matthews, E.: Global methane emissions from landfills: New methodology and
932 annual estimates 1980–1996, Global Biogeochem. Cycles, 17(2), 1065,
933 https://doi.org/10.1029/2002GB001913, 2003.

934 Bogner, J., Pipatti, R., Hashimoto, S., Diaz, C., Mareckova, K., Diaz, L., Kjeldsen, P., Monni, S.,
935 Faaij, A., Qingxian, G., Tianzhu, Z., Mohammed, A. A., Sutamihardja, R. T. M., and Gregory, R.:
936 Mitigation of global greenhouse gas emissions from waste: Conclusions and strategies from the
937 Intergovernmental Panel on Climate Change (IPCC) Fourth Assessment Report, Waste Manag.
938 Res., 26(1), 11–32, https://doi.org/10.1177/0734242X07088433, 2008.

939 Boisier, J. P., Marinao, R., and Alvarez Garreton, C.: CR2LUC: Historical (1950–2020) land use
940 and land cover in continental Chile (v1.0), Zenodo [data set],
941 https://doi.org/10.5281/zenodo.13324250, 2024a.

942 Boisier, J. P., Marinao, R., and Alvarez Garreton, C.: CR2WU: Water use dataset for the period
943 1950–2020 in continental Chile (v1.0), Zenodo [data set],
944 https://doi.org/10.5281/zenodo.13324235, 2024b.

945 Carbon Mapper: Carbon Mapper Emissions Data Explorer, https://data.carbonmapper.org/, last
946 access: 15 September 2025, 2025.

947 Castesana, P. S., Dawidowski, L. E., Finster, L., Gómez, D. R., and Taboada, M. A.: Ammonia
948 emissions from the agriculture sector in Argentina; 2000–2012, Atmos. Environ., 178, 293–304,
949 https://doi.org/10.1016/j.atmosenv.2018.02.003, 2018.

https://doi.org/10.5194/essd-2026-850
Preprint. Discussion started: 13 November 2026
© Author(s) 2026. CC BY 4.0 License.



950 Cayumil, R., Khanna, R., Konyukhov, Y., Burmistrov, I., Kargin, J. B., and Mukherjee, P. S.: An
951 overview on solid waste generation and management: Current status in Chile, Sustain., 13(21),
952 11644, https://doi.org/10.3390/su132111644, 2021.

953 Crippa, M., Guizzardi, D., Pagani, F., Schiavina, M., Melchiorri, M., Pisoni, E., Graziosi, F.,
954 Muntean, M., Maes, J., Dijkstra, L., Van Damme, M., Clarisse, L., and Coheur, P.: Insights into
955 the spatial distribution of global, national, and subnational greenhouse gas emissions in the
956 Emissions Database for Global Atmospheric Research (EDGAR v8.0), Earth Syst. Sci. Data,
957 16(6), 2811–2830, https://doi.org/10.5194/essd-16-2811-2024 , 2024.

958 Dangal, S. R. S., Tian, H., Zhang, B., Pan, S., Lu, C., and Yang, J.: Methane emission from global
959 livestock sector during 1890–2014: Magnitude, trends and spatiotemporal patterns, Glob. Change
960 Biol., 23(10), 4147–4161, https://doi.org/10.1111/gcb.13709, 2017.

961 European Environment Agency: EMEP/EEA air pollutant emission inventory guidebook 2023:
962 Technical guidance to prepare national emission inventories (EEA Report No. 06/2023), European
963 Environment Agency, https://doi.org/10.2800/795737, 2023.

964 Food and Agriculture Organization of the United Nations (FAO): Methane emissions in livestock
965 and rice systems: Sources, quantification, mitigation and metrics, Food and Agriculture
966 Organization of the United Nations, Rome, Italy, https://doi.org/10.4060/cc7607en, 2023.

967 Huneeus, N., Denier van der Gon, H., Castesana, P., Menares, C., Granier, C., Granier, L., Alonso,
968 M., de Fatima Andrade, M., Dawidowski, L., Gallardo, L., Gomez, D., Klimont, Z., Janssens-
969 Maenhout, G., Osses, M., Puliafito, S. E., Rojas, N., Ccoyllo, O. S., Tolvett, S., and Ynoue, R. Y.:
970 Evaluation of anthropogenic air pollutant emission inventories for South America at national and
971 city scale, Atmos. Environ., 235, https://doi.org/10.1016/j.atmosenv.2020.117606, 2020.

972 Instituto Nacional de Estadísticas (INE): Estimates and projections of the population in Chile
973 2002–2035: communal totals, urban and rural population, Instituto Nacional de Estadísticas de
974 Chile, https://www.ine.gob.cl/estadisticas/sociales/demografia-y-vitales/proyecciones-de-
975 poblacion, 2017a.

976 Instituto Nacional de Estadísticas (INE): 2017 Census Cartography: Census blocks and entities
977 [shapefile], Instituto Nacional de Estadísticas de Chile,
978 https://www.ine.gob.cl/herramientas/portal-de-mapas/geodatos-abiertos, last access: 20
979 September 2025, 2017b.

980 Instituto Nacional de Estadísticas (INE): Boletín Ferias y Mataderos, trimestre julio–septiembre
981 2025, Instituto Nacional de Estadísticas, Gobierno de Chile, https://www.ine.gob.cl/docs/default-

https://doi.org/10.5194/essd-2026-850
Preprint. Discussion started: 13 November 2026
© Author(s) 2026. CC BY 4.0 License.



source/mataderos-de-ganado/boletines/feria-y-mataderos/bolet%C3%ADn-ferias-y-mataderos-trimestre-julio-septiembre-2025.pdf?sfvrsn=afff3c14_4, 2025.

Intergovernmental Panel on Climate Change (IPCC): 2006 IPCC guidelines for national greenhouse gas inventories, Prepared by the National Greenhouse Gas Inventories Programme, edited by H. S. Eggleston, L. Buendia, K. Miwa, T. Ngara, and K. Tanabe, IGES, Japan, https://www.ipcc-nggip.iges.or.jp/public/2006gl/index.html, 2006.

Intergovernmental Panel on Climate Change (IPCC): 2019 refinement to the 2006 IPCC guidelines for national greenhouse gas inventories, edited by E. Calvo Buendía, K. Tanabe, A. Kranjc, J. Baasansuren, M. Fukuda, S. Ngarize, A. Osako, Y. Pyrozhenko, P. Shermanau, and S. Federici, IPCC, https://www.ipcc.ch/report/2019-refinement-to-the-2006-ipcc-guidelines-for-national-greenhouse-gas-inventories/, 2019.

Intergovernmental Panel on Climate Change (IPCC): Summary for Policymakers, in: Climate Change 2021: The Physical Science Basis, Contribution of Working Group I to the Sixth Assessment Report of the Intergovernmental Panel on Climate Change, edited by V. Masson-Delmotte, P. Zhai, A. Pirani, S. L. Connors, C. Péan, S. Berger, N. Caud, Y. Chen, L. Goldfarb, M. I. Gomis, M. Huang, K. Leitzell, E. Lonnoy, J. B. R. Matthews, T. K. Maycock, T. Waterfield, O. Yelekçi, R. Yu, and B. Zhou, Cambridge University Press, Cambridge, United Kingdom and New York, NY, USA, 3–32, https://doi.org/10.1017/9781009157896.001, 2021.

Ishigaki, T., Yamada, M., Nagamori, M., Ono, Y., & Inoue, Y.: Estimation of methane emission from a whole waste landfill site using correlation between flux and ground temperature. Environ. Geol., 48, 845–853. https://doi.org/10.1007/s00254-005-0008-0, 2005.

Kaza, S., Yao, L. C., Bhada-Tata, P., Van Woerden, F., and Levine, D. C.: What a Waste 2.0: A Global Snapshot of Solid Waste Management to 2050, Urban Development, World Bank, Washington, DC, https://doi.org/10.1596/978-1-4648-1329-0, 2018.

Malmir, T., Lagos, D., and Eicker, U.: Optimization of landfill gas generation based on a modified first-order decay model: a case study in the province of Quebec, Canada, Environ. Sys. Res., 12(6), https://doi.org/10.1186/s40068-023-00292-w, 2023.

Merab, P. B. N., Sadoth, S. T., and Isidro, B. J. S.: First-Order Decay Models for the Estimation of Methane Emissions in a Landfill in the Metropolitan Area of Oaxaca City, Mexico, Waste, 3(2), 14, https://doi.org/10.3390/waste3020014, 2025.

Ministerio del Medio Ambiente (MMA): Reporte del Estado del Medio Ambiente 2023, Sistema Nacional de Información Ambiental (SINIA), Gobierno de Chile, available at:

https://doi.org/10.5194/essd-2026-850
Preprint. Discussion started: 13 November 2026
© Author(s) 2026. CC BY 4.0 License.



https://sinia.mma.gob.cl/estado-del-medio-ambiente/reporte-del-estado-del-medio-ambiente-2023/, last access: 7 October 2025, 2023.

Ministerio del Medio Ambiente (MMA): Documento del Inventario Nacional de Gases de Efecto Invernadero de Chile, serie 1990–2022, Gobierno de Chile, https://snichile.mma.gob.cl/wp-content/uploads/2025/03/2024_DIN_CL.pdf, 2024a.

Ministerio del Medio Ambiente (MMA): Registro de Emisiones y Transferencia de Contaminantes (RETC) – Residuos, available at: https://datosretc.mma.gob.cl/group/residuos, last access: 18 April 2025, 2024b.

Ministerio del Medio Ambiente (MMA): Landfill methane recovery data by disposal site in Chile, unpublished data obtained via direct institutional request, Ministerio del Medio Ambiente, Santiago, Chile, 2024c.

Ministerio de Desarrollo Social y Familia (MDSF): Encuesta de Caracterización Socioeconómica Nacional (CASEN) [olas 2006, 2009, 2011, 2013, 2015, 2017, 2020, 2022], Observatorio Social, Santiago, Chile, available at: https://observatorio.ministeriodesarrollosocial.gob.cl/encuesta-casen, last access: 12 April 2025, 2024.

Ministerio de Planificación y Cooperación (MIDEPLAN): Empalme de las series de PIB regional 1960–2001 (Anexo), Gobierno de Chile, available at: https://www.desarrollosocialyfamilia.gob.cl/btca/txtcompleto/mideplan/empalme-seriepibreg.1960-2001final-anexo.pdf, last access: 12 September 2025, 2004.

Morales P., R. and Martínez P., M. E.: Transición hacia la ganadería sostenible en Chile: Protegiendo la seguridad y soberanía alimentaria y agregando valor a los productos pecuarios, in: Libro de resúmenes de la reunión del equipo de ganadería INIA: Generación de una estrategia para la transición hacia una ganadería sostenible y sustentable, edited by: Morales P., R., Martínez P., M. E., Moscoso J., C., and Subiabre R., I., Serie Actas INIA No. 67, 59–65, Instituto de Investigaciones Agropecuarias (INIA), Osorno, Chile, available at: https://biblioteca.inia.cl/entities/acta/3a8130ad-942d-4e48-94b0-e52245d2ce3f, 2025.

Oficina de Estudios y Políticas Agrarias (ODEPA): Estadísticas silvoagropecuarias y económicas del sector agropecuario-silvícola en Chile, Ministerio de Agricultura, Gobierno de Chile, available at: https://www.odepa.gob.cl, last access: 12 September 2025, 2024.

Osses, M., Rojas, N., Ibarra, C., Valdebenito, V., Laengle, I., Pantoja, N., Osses, D., Basoa, K., Tolvett, S., Huneeus, N., Gallardo, L., and Gómez, B.: High-resolution spatial-distribution maps

https://doi.org/10.5194/essd-2026-850
Preprint. Discussion started: 13 November 2026
© Author(s) 2026. CC BY 4.0 License.



of road transport exhaust emissions in Chile, 1990–2020, Earth Syst. Sci. Data, 14, 1359–1376, https://doi.org/10.5194/essd-14-1359-2022, 2022.

Petrescu, A. M. R., Peters, G. P., Engelen, R., Houweling, S., Brunner, D., Tsuruta, A., Matthews, B., Patra, P. K., Belikov, D., Thompson, R. L., Höglund-Isaksson, L., Zhang, W., Segers, A. J., Etiope, G., Ciotoli, G., Peylin, P., Chevallier, F., Aalto, T., Andrew, R. M., Bastviken, D., Berchet, A., Broquet, G., Conchedda, G., Dellaert, S. N. C., Denier van der Gon, H., Gütschow, J., Haussaire, J.-M., Lauerwald, R., Markkanen, T., van Peet, J. C. A., Pison, I., Regnier, P., Solum, E., Scholze, M., Tenkanen, M., Tubiello, F. N., van der Werf, G. R., and Worden, J. R.: Comparison of observation- and inventory-based methane emissions for eight large global emitters, Earth Syst. Sci. Data, 16, 4325–4350, https://doi.org/10.5194/essd-16-4325-2024, 2024.

Puliafito, S. E., Bolaño-Ortiz, T. R., Fernandez, R. P., Berná, L. L., Pascual-Flores, R. M., Urquiza, J., López-Noreña, A. I., and Tames, M. F.: High-resolution seasonal and decadal inventory of anthropogenic gas-phase and particle emissions for Argentina, Earth Syst. Sci. Data, 13, 5027–5069, https://doi.org/10.5194/essd-13-5027-2021, 2021.

Reisinger, A., Clark, H., Cowie, A. L., Emmet-Booth, J., Gonzalez Fischer, C., Herrero, M., Howden, M., and Leahy, S.: How necessary and feasible are reductions of methane emissions from livestock to support stringent temperature goals?, Philos. Trans. R. Soc. A, 379, 20200452, https://doi.org/10.1098/rsta.2020.0452, 2021.

Sarricolea, P., Herrera-Ossandon, M., and Meseguer-Ruiz, Ó.: Climatic regionalisation of continental Chile, J. Maps, 13, 66–73, https://doi.org/10.1080/17445647.2016.1259592, 2017.

Saunois, M., Martinez, A., Poulter, B., Zhang, Z., Raymond, P. A., Regnier, P., Canadell, J. G., Jackson, R. B., Patra, P. K., Bousquet, P., Ciais, P., Dlugokencky, E. J., Lan, X., Allen, G. H., Bastviken, D., Beerling, D. J., Belikov, D. A., Blake, D. R., Castaldi, S., Crippa, M., Deemer, B. R., Dennison, F., Etiope, G., Gedney, N., Höglund-Isaksson, L., Holgerson, M. A., Hopcroft, P. O., Hugelius, G., Ito, A., Jain, A. K., Janardanan, R., Johnson, M. S., Kleinen, T., Krummel, P. B., Lauerwald, R., Li, T., Liu, X., McDonald, K. C., Melton, J. R., Mühle, J., Müller, J., Murguia-Flores, F., Niwa, Y., Noce, S., Pan, S., Parker, R. J., Peng, C., Ramonet, M., Riley, W. J., Rocher-Ros, G., Rosentreter, J. A., Sasakawa, M., Segers, A., Smith, S. J., Stanley, E. H., Thanwerdas, J., Tian, H., Tsuruta, A., Tubiello, F. N., Weber, T. S., van der Werf, G. R., Worthy, D. E. J., Xi, Y., Yoshida, Y., Zhang, W., Zheng, B., Zhu, Q., Zhu, Q., and Zhuang, Q.: Global Methane Budget 2000–2020, Earth Syst. Sci. Data, 17, 1873–1958, https://doi.org/10.5194/essd-17-1873-2025, 2025.

https://doi.org/10.5194/essd-2026-850
Preprint. Discussion started: 13 November 2026
© Author(s) 2026. CC BY 4.0 License.



1077 Servicio Agrícola y Ganadero (SAG): Establishment records for high-intensity livestock systems
1078 in Chile, unpublished administrative data obtained via Chilean Transparency Law request,
1079 Servicio Agrícola y Ganadero, Santiago, Chile, 2024.

1080 Spokas, K., Graff, C., Morcet, M., and Aran, C.: Implications of the spatial variability of landfill
1081 emission rates on geospatial analyses, Waste Manage., 23, 599–607,
1082 https://doi.org/10.1016/S0956-053X(03)00102-8, 2003.

1083 Subsecretaría de Desarrollo Regional y Administrativo (SUBDERE): Diagnóstico y catastro de
1084 los residuos sólidos domiciliarios a nivel nacional 2012, Subsecretaría de Desarrollo Regional y
1085 Administrativo, Santiago, Chile, 2013.

1086 Subsecretaría de Desarrollo Regional y Administrativo (SUBDERE): Línea base diagnóstico y
1087 catastro de residuos sólidos domiciliarios, captura año 2017, Subsecretaría de Desarrollo Regional
1088 y Administrativo, Santiago, Chile, https://proactiva.subdere.gov.cl/handle/123456789/518, 2018.

1089 Subsecretaría de Desarrollo Regional y Administrativo (SUBDERE): Estudio de caracterización
1090 de los residuos sólidos domiciliarios y asimilables generados a nivel municipal en Chile: Informe
1091 Final Consolidado, Subsecretaría de Desarrollo Regional y Administrativo, Santiago, Chile,
1092 https://proactiva.subdere.gov.cl/handle/123456789/649, 2024.

1093 Superintendencia de Servicios Sanitarios (SISS): Informes de coberturas del sector sanitario
1094 [informes anuales 2005–2022], Superintendencia de Servicios Sanitarios, Gobierno de Chile,
1095 available at: https://www.siss.gob.cl/589/w3-propertyvalue-8979.html, last access: 4 April 2025,
1096 2024a.

1097 Superintendencia de Servicios Sanitarios (SISS): Operational wastewater data (treated volumes,
1098 BOD, sludge and treatment plant locations), 2005–2022, unpublished administrative data obtained
1099 via Chilean Transparency Law request, Santiago, Chile, 2024b.

1100 United Nations Environment Programme and Climate and Clean Air Coalition (UNEP/CCAC):
1101 Global Methane Assessment: Benefits and Costs of Mitigating Methane Emissions, United
1102 Nations Environment Programme, Nairobi, https://wedocs.unep.org/items/4d9774f8-1a9d-42d1-
1103 be2c-122408159b15, 2021.

1104 United Nations Framework Convention on Climate Change (UNFCCC): National Inventory
1105 Submissions 2023, UNFCCC, available at: https://unfccc.int/ghg-inventories-annex-i-
1106 parties/2023, last access: 12 September 2025, 2023.

https://doi.org/10.5194/essd-2026-850
Preprint. Discussion started: 13 November 2026
© Author(s) 2026. CC BY 4.0 License.



1107 World Bank: GDP (current US$) – Chile, World Development Indicators, available at:
1108 https://data.worldbank.org/indicator/NY.GDP.MKTP.CD?locations=CL, last access: 12
1109 September 2025, 2024.

1110